СИБИРСКОЕ ОТДЕЛЕНИЕ
РОССИЙСКОЙ АКАДЕМИИ НАУК

НАУЧНЫЙ ЖУРНАЛ
ГЕОЛОГИЯ И ГЕОФИЗИКА

Геология и геофизика, 2016, т. 57, № 10, с. 1784—1807

УДК 551.24(560/566)

ХИМИЯ ВАЛОВЫХ ПОРОД И МИНЕРАЛОВ МАФИТОВЫХ КУМУЛАТОВ НИЗКОТИТАНОВОГО ОФИОЛИТА В ЮЖНОЙ ЧАСТИ КАХРАМАНМАРАША (*Турция*)

М. Танирли, Т. Ризаоглу

Kahramanmaraş Sütçü İmam University, Department of Geological Engineering, TR46100 Kahramanmaraş-TURKEY

Позднемеловая расчленённая офиолитовая толща в южной части Кахраманмараша является частью Арабского офиолитового пояса, расположенного в южной Турции. Офиолитовый разрез включает (снизу вверх) метаморфическую подошву (плагиоклаз-амфиболовый сланец и плагиоклазовый амфиболит), мантийные тектониты (серпентинизированный дунит и гарцбургит), ультрамафитовые кумулаты (преимущественно вебстерит), мафические кумулаты (оливиновое габбро, габбро и оливиновый габбронорит) и изотропное габбро (оливиновый габбронорит). По геохимическому составу валовые породы кумулатов можно классифицировать как низкотитановый офиолит и его производные, образовавшиеся из островодужной толеитовой магмы. Нормализованные на хондрит диаграммы РЗЭ, нормализованные на N-MORB многоэлементные диаграммы и тектономагматические дискриминационные диаграммы показывают важную роль фракционной кристаллизации в образовании кумулятивных пород. Присутствие высокомагнезиальных оливинов ($Fo_{78.24-81.89}$), клинопироксенов ($Mg\#_{71.46-85.82}$), ортопироксенов ($Mg\#_{62.63-87.18}$) и высококальциевых плагиоклазов ($An_{81.88-97.40}$) в мафитовых кумулатах свидетельствует об их образовании в обстановке, связанной с субдукционными процессами. Полученные геохимические и петрографические данные и результаты полевых работ показывают, что изученные офиолитовые породы, вероятно, образовались в надсубдукционной обстановке в южной части Неотетиса в позднемеловую эпоху.

Надсубдукционная обстановка, низкотитановый офиолит, кумулат, Кахраманмараш, Турция.

WHOLE-ROCK AND MINERAL CHEMISTRY OF MAFIC CUMULATES FROM THE LOW-Ti OPHIOLITE IN THE SOUTHERN PART OF KAHRAMANMARAŞ, TURKEY

M. Tanirli and T. Rızaoğlu

A Late Cretaceous dismembered ophiolite unit in the south of Kahramanmaraş belongs to the Peri-Arabian ophiolite belt in southern Turkey. The ophiloitic rocks include, from bottom to top, metamorphic sole (plagioclase–amphibole schist and plagioclase amphibolite), mantle tectonites (serpentinized dunite and harzburgite), ultramafic cumulates (mainly websterite), mafic cumulates (olivine gabbro, gabbro, and olivine gabbronorite), and isotropic gabbros (olivine gabbronorite). The whole-rock geochemistry of the cumulates suggests that they can mainly be classified as Low-Ti ophiolite and cumulate rocks derived from an island-arc tholeiitic magma source. Chondrite-normalized REE and N-MORB-normalized multielement patterns and tectonomagmatic discrimination diagrams show that fractional crystallization was important during the formation of the cumulate rocks. The presence of highly magnesian olivines ($Fo_{78.24-81.89}$), clinopyroxenes ($Mg\#_{71.46-85.82}$), and orthopyroxenes ($Mg\#_{62.63-87.18}$) as well as highly calcic plagioclases ($An_{81.88-97.40}$) in the mafic cumulates indicates a subduction-related tectonic environment. The geochemical, petrographical, and field data suggest that the ophiolitic rocks in the studied region formed in a suprasubduction zone environment in the southern branch of Neotethys in the Late Cretaceous.

Suprasubduction, *Low*-Ti *ophiolite, cumulate, Kahramanmaraş, Turkey*

1. INTRODUCTION

Turkey is located in a critical segment along the Alpine-Himalayan orogenic system, where ophiolitic bodies representing the remnants of the Neotethys are generally characterized in a structural descending order by ophiolites, metamorphic soles and ophiolitic melanges as the members of the suture zones of Anatolia (Şengör and Yılmaz, 1981; Yılmaz et al., 1993; Robertson, 2002). These suture zones, from north to south, are the Intra-Pontide (Şengör and Yılmaz, 1981; Okay, 1989; Yılmaz et al., 1997; Okay and Tüysüz, 1999), the İzmir-Ankara-Erzincan suture (Şengör and Yılmaz, 1981), the Inner Tauride suture (Görür et al., 1984) and the

✉e-mail:tamer@ksu.edu.tr
DOI: 10.15372/GiG20161003

South-east Anatolian suture zones (Şengör and Yılmaz, 1981; Yılmaz, 1993; Yılmaz et al., 1993; Robertson et al., 2006; 2007). The Neotethyan ophiolites in Turkey are located mainly in E-W trending five belts. These are namely the Tauride ophiolites, the Central Anatolian ophiolites, the Pontide ophiolites, the southeast Anatolian ophiolites and the Peri-Arabian ophiolite belt (Fig. 1). The ophiolitic rocks to the south of Kahramanmaraş is located in the Peri-Arabian ophiolite belt (Fig. 1) and can be correlated with the Koçali ophiolite in the east and the Kızıldağ (Hatay) the Troodos ophiolites in the southwest along the Bitlis-Zagros suture.

For several years, ophiolitic units have been regarded as the obducted slices of the oceanic lithosphere, generated at the mid-ocean ridges (Gass, 1968, 1990; Coleman, 1977) or suprasubduction zones (Miyashiro, 1973, 1975; Pearce et al., 1981, 1984). The Mesozoic ophiolites in the Alpine-Himalayan belt formed in various tectonic settings, including subduction related (Eastern Albanian and Vourinos ophiolites in Greece), MORB (Western Albanian ophiolites), transitional from MORB to SSZ (South Albanian ophiolites, Pindos and Asproptamos ophiolites in Greece) and intracontinental back-arc basin (Guevgueli ophiolite in NE Greece) (Robertson, 2002 and references therein; Hoeck et al., 2002). The Late Cretaceous ophiolites in Turkey, Troodos in Cyprus and Baer-Bassit in Syria were formed in a suprasubduction zone (SSZ) tectonic setting (Aktaş and Robertson, 1984; Pearce et al., 1984; Hébert and Laurent, 1990; Lytwyn and Casey, 1995; Yalınız et al., 1996; Collins and Robertson, 1998; Beyarslan and Bingöl, 2000; Floyd et al., 2000; Parlak et al., 1996, 2000, 2002, 2004, 2009; Al-Riyami et al., 2002; Robertson, 2002; Bağcı et al., 2005, 2006; Rızaoğlu et al., 2006; Bağcı et al., 2008; Bağcı and Parlak, 2009; Bağcı, 2013).

Serri (1980) divided the ophiolites into two groups namely the low- and high-Ti ophiolites. The high-Ti ophiolites are more akin to mid-ocean ridge basalt (MORB)-like magma, whereas the low-Ti ophiolites have a spectrum of composition changing from mid ocean ridge basalts (MORB) to Island Arc Tholeiites (IAT) and boninite-like magmas (Serri, 1980).

In this paper we present petrographical and geochemical (whole rock and mineral chemistry) characteristics of the gabbroic cumulates from a poorly-known ophiolite body in SE Turkey in order to better understand (a) geodynamic environment of formation, (b) their correlation with the well-known ophiolites and (c) their importance within the eastern Mediterranean tectonic frame.

2. GEOLOGICAL SETTING

The basement of the geological units in the region is represented by Lower Cambrian-Upper Ordovician Arabian autochthonous units consisting of alternation of limestone, sandstone, quartzite and shale (Fig. 2). This basement unit is uncorfomably overlain by the Upper Triassic-Lower Cretaceous carbonates (Dubertret, 1955; Atan, 1969; Yılmaz et al., 1984; Tekeli and Erendil, 1986; Bağcı, 2013). The Arabian platform is tectonically

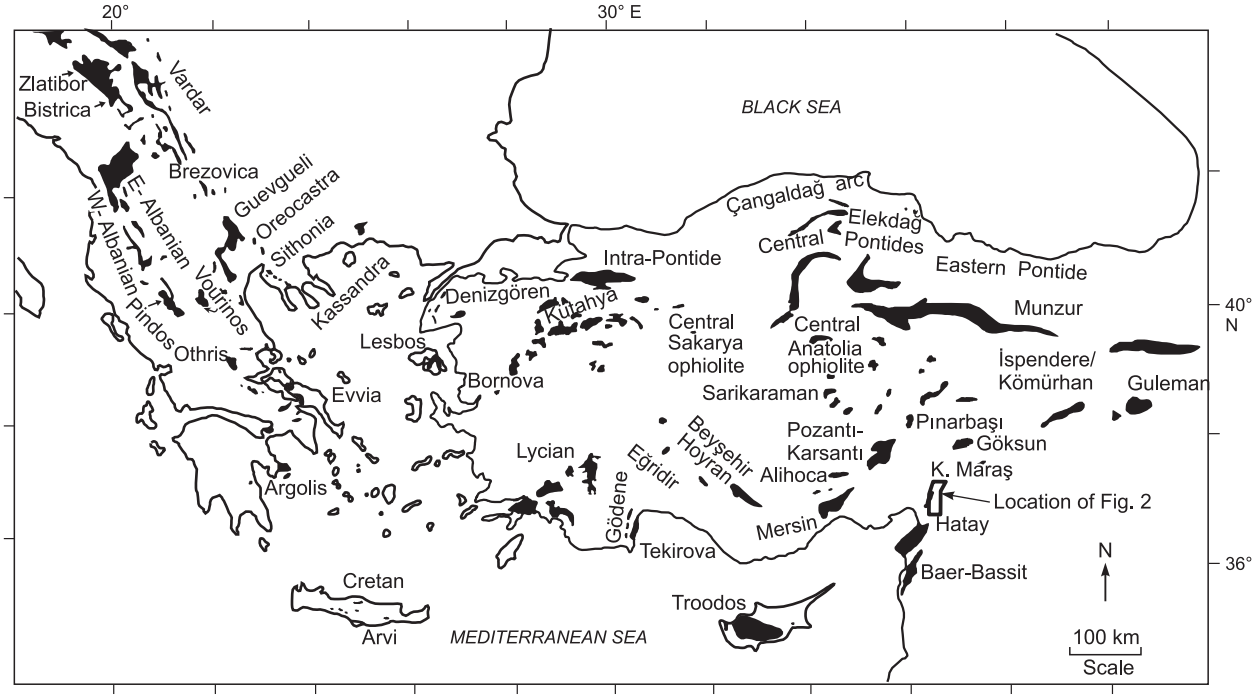

Fig. 1. Distribution of the Neotethyan ophiolites in the eastern Mediterranean region (from Robertson 2002).

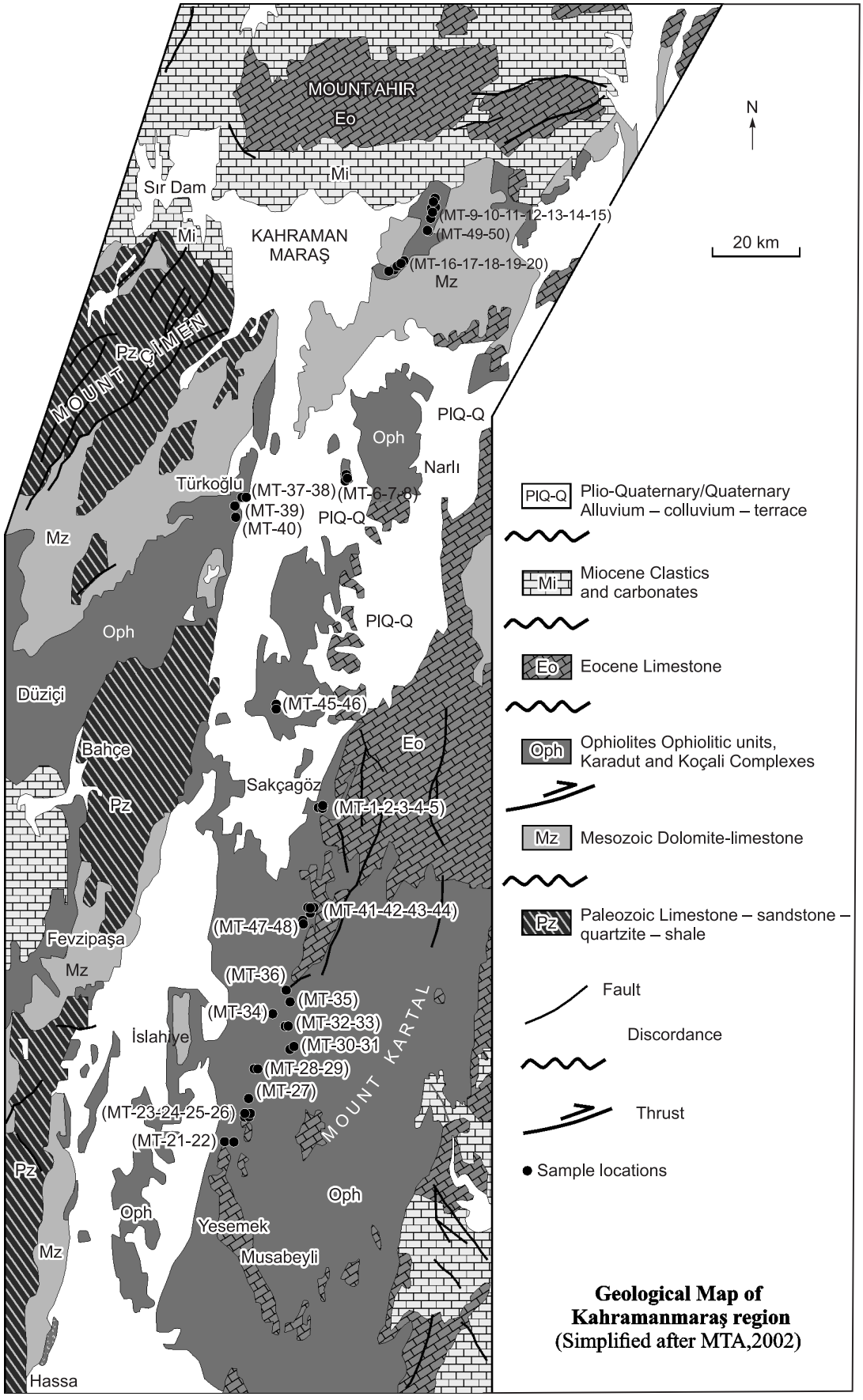

Fig. 2. Regional geological map of the Kahramanmaraş region (Simplified after MTA, 2002).

overlain by a group of oceanic basin units such as Karadut complex, Koçali complex and ophiolitic units (Yılmaz et al., 1993) (Fig. 2). The Karadut Complex is named by Turkish oil company geologists (after Tuna, 1973) , and is mainly composed of moderately metamorphosed units such as red, green or reddish green silicified limestone, siliceous shale, marl interbedded crystallized limestone, and radiolarite (Sungurlu, 1974; Yalçın, 1979). The Koçali complex includes the Koçali Ophiolite and the volcanic-sedimentary Koçali melange. The ophiolitic rocks form E-W trending thrust sheets in which all of the components of a complete ophiolite sequence are present, although mainly separated by tectonic contacts; i.e. (from bottom to top), serpentinised harzburgite, layered cumulates, isotropic gabbros, sheeted dykes, pillow lavas, radiolarian and metalliferous sediments (Yıldırım et al., 2012). The studied ophiolitic rocks in the region overlie the Koçali and Karadut complexes and are unconformably overlain by the Late Maastrichtian-Paleocene sedimentary rocks. The Koçali complex is also composed of the alternations of limestone, sandstone, siltstone and mudstone (Sungurlu, 1974; Erdoğan, 1975; Yalçın, 1979; Bağcı, 2013) (Fig. 1). Allochthonous units in the region are emplaced onto the Arabian platform in Late Cretaceous (Koçali and Karadut complexes), and in Miocene (Malatya metamorphics, Andırın Limestone, and Berit metaophiolite) (Yılmaz et al., 1987; Gül, 2000).

The ophiolitic rocks in the region start at the bottom with the metamorphic sole rocks. The metmorphic sole rocks are metamorphosed from green schist to amphibolite facies. Then the unit passes into the mantle tectonites, ultramafic to mafic cumulates and isotropic gabbros. The contacts between the sub-units of the ophiolite are tectonic. The Upper Paleocene-Miocene sedimentary units unconformably overlie the older units in the region (Gül, 1987; Terlemez et al., 1992; Bağcı, 2013). In turn, those units are covered by the Yavuzeli basalts Tortonian in age (Yoldemir, 1987). Upper Paleocene-Holocene units cover all the previously formed units with angular unconformity (Fig. 2).

3. PETROGRAPHY

The ophiolite related rocks in the study area are represented by metamorphic sole rocks, mantle tectonites, ultramafic cumulate rocks, mafic cumulate rocks and isotropic gabbroic rocks. The lowest unit in the region is metamorphic sole unit and is tectonically overlain by mantle tectonites. The mantle tectonites are seen as strongly sheared and deformed in the field (Fig. 3a). The mantle tectonites host the podiform chromite deposits. The tectonites pass into ultramafic to mafic cumulates showing typical characteristics of cumulate textures such

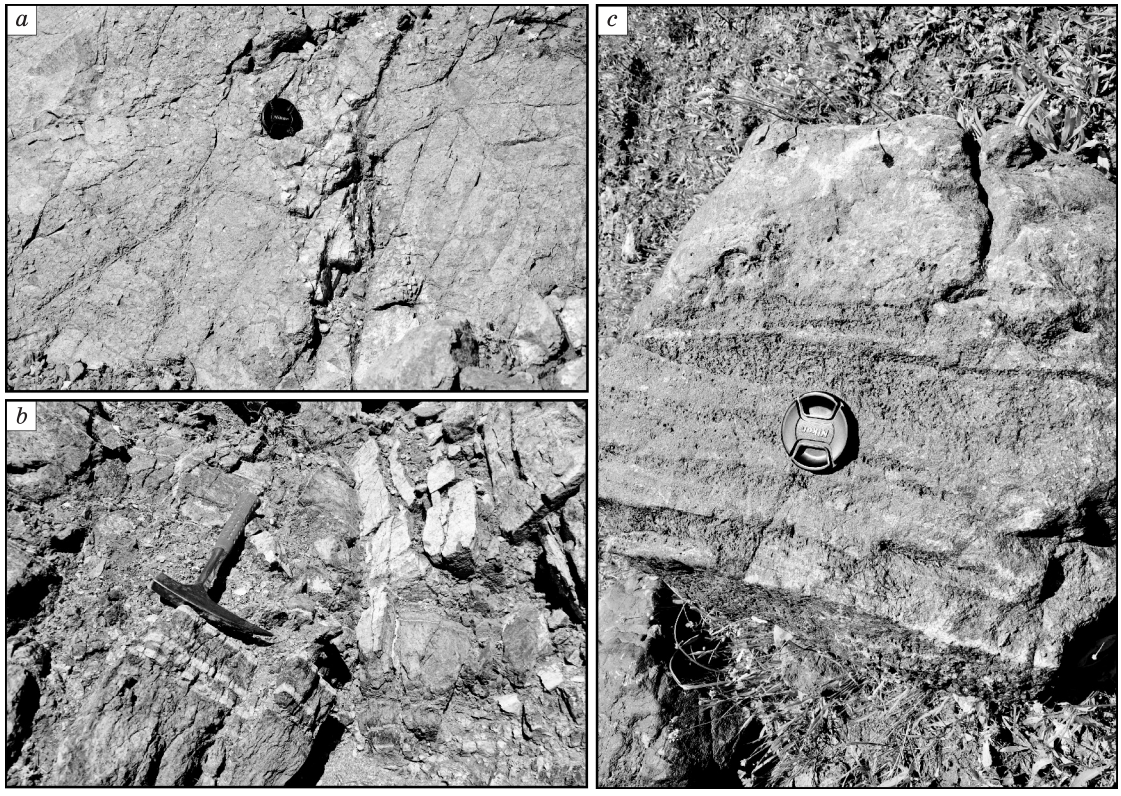

Fig. 3. Field views from the different ophiolitic units. (*a*) Sheared and serpentinized mantle tectonites (*b*) cumulate texture from the ultramafic cumulates (*c*) Cumulate texture and crossed bedding from mafic cumulates.

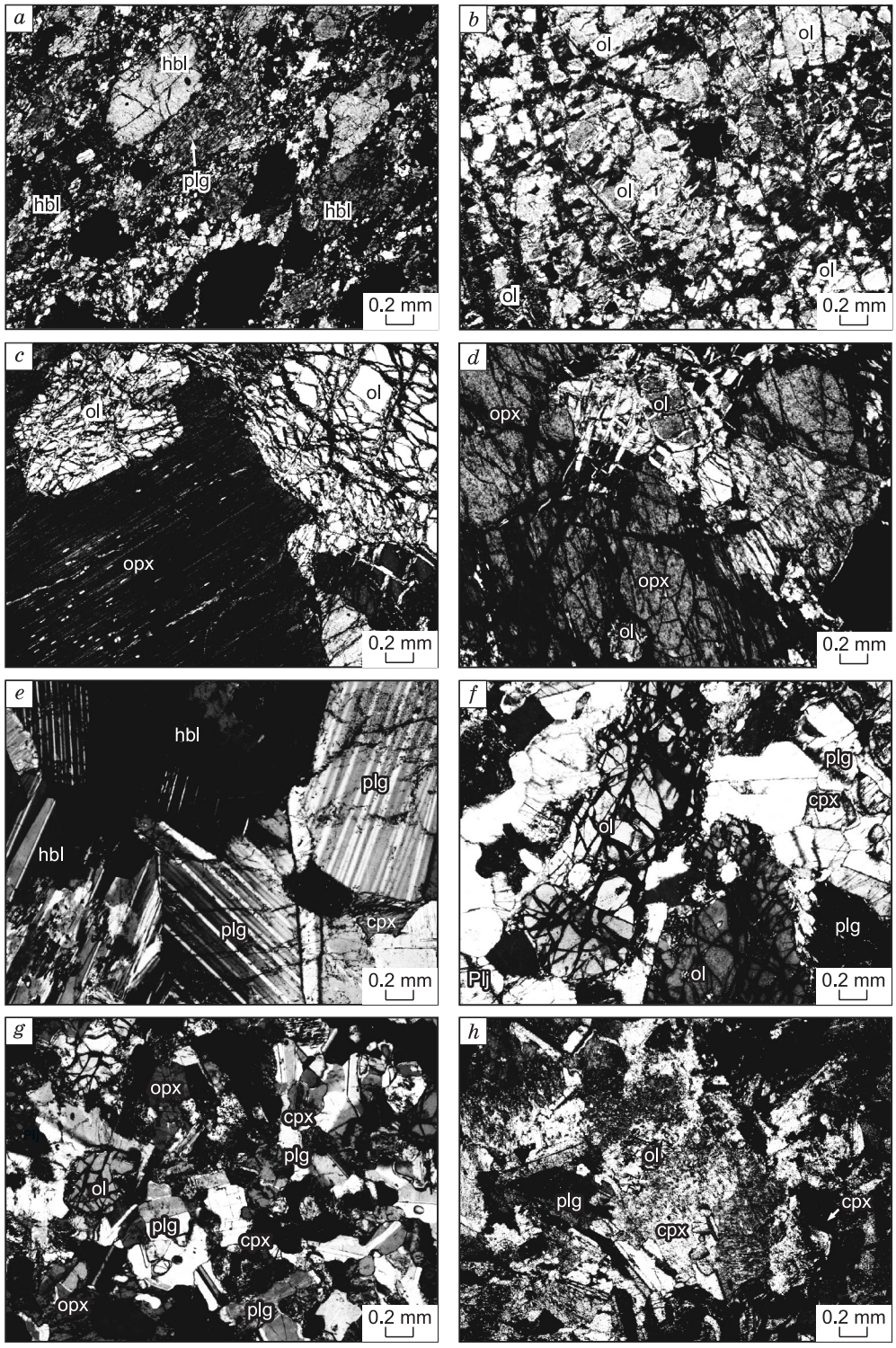

Fig. 4. Petrographic views of the rocks from the ophiolitic units:

(*a*) Nematoblastic texture in plagioclase-amphibole schist (*b*) granular and mesh texture in dunite (tectonites); (*c*) poikilitic texture in lherzolite from ultramafic cumulates; (*d*) poikilitic and granular texture in harzburgite from the ultramafic cumulates; (*e*) general view of cumulate gabbro; (*f*) granular texture in cumulate olivine gabbro; (*g*), general view from the cumulate olivine gabbronorite; (*h*) granular texture in olivine gabbronorite (isotrop gabbro). Abbreviations: *ol* olivine, *opx* orthopyroxene, *cpx* clinopyroxene, *plg* plagioclase, *hbl* hronblende

as magmatic banding, layering, crossed bedding and grading (Fig. 3b,c). The highest level of the ophiolite in the region is represented by isotropic gabbros.

The formation of the metamorphic sole rocks beneath the ophiolite section was described by Williams and Smyth (1973) in Newfounland ophiolite in Canada. Later on, the existence and the development of a sole with an inverted metamorphic zonation situated below tectonites in many other ophiolites published by different authors (Jameison, 1979; Nicolas, 1989; Peacock and Norris, 1989; Gnos and Peters, 1993; Sandeman et al., 1995; Parlak et al., 1995; Parlak and Delaloye, 1999).

The metamorphic sole rocks crop out in the southeastern end of the study area especially in the eastern part of Kahramanmaraş (Fig. 2). The unit is represented by plagioclase-amphibole schist and plagioclase amphibolite. The plagioclase-amphibole schist exhibits nematoblastic, banded to poikiloblastic textures and comprise plagioclase (15-20 vol. %), amphibole (70-75 vol. %), chlorite, epidote, titanite and magnetite (Fig. 4a). The plagioclase amphibolites show granoblastic to grano-nematoblastic texture and are represented by plagioclase (20-25 vol. %), amphibole (70-75 vol. %), muscovite (2-3 vol. %) and accessory sphene and magnetite minerals.

Mantle tectonites are the most extensive rocks within the ophiolites in the region and are of dunite, serpentinized dunite, serpentinized harzburgite, and serpentinite. The dunites show granular texture and are composed of olivine (97-98 vol. %) and rare chromite crystals are set in partly serpentinized olivines and orthopyroxenes (Fig. 4b). The serpentinized dunites show mesh to granular textures and are mainly composed of olivine (90-95 vol. %), clinopyroxene (1-2 vol. %) and chromite. The serpentinized harzburgites exhibit granular to mesh textures, and are composed of olivine (~ 80 vol. %), orthopyroxene (~ 15 vol. %) and opaque minerals (magnetite and chromite). The serpentinites are represented by mest texture and mainly composed of serpentine group minerals (chrysotile and bastite).

The ultramafic to mafic cumulate rocks crop out mostly in the vicinity of Narlı and Nurdağı towns (Fig. 2). The ultramafic cumulates consist of lherzolite, serpentinized harzburgite, and websterite, whereas the mafic cumulates are represented by gabbro, olivine gabbro, and olivine gabbronorite. The lherzolite shows granular, poikilitic and mesh textures and is characterized by olivine (55-60 % vol), orthopyroxene (20-25 vol. %), clinopyroxene (10-15 vol. %) and chromite (Fig. 4c). The serpentinized harzburgite displays granular, poikilitic and mesh textures and is represented by olivine (70-80 % vol), orthopyroxene (20-25 vol. %), clinopyroxene (2-3 vol. %) and chromite (1-2 vol. %). The olivines and pyroxenes in the harzburgites are serpentinized to variable degrees (Fig. 4d). The websterite displays granular texture and is represented by two kinds of pyroxenes with variable amounts. The opaque mineral phase is represented by magnetite occurrences. The gabbro displays granular to poikilitic textures and is characterized by plagioclase (70-75 vol. %), clinopyroxene (15-20 vol. %), amphibole (4-5 vol.%), olivine (1-2 vol. %), and orthopyroxene (1-2 vol. %). Kaolin, sericite, chlorite and magnetite are secondary phases (Fig. 4e). The olivine gabbro displays granular to poikilitic textures: it contains plagioclase (55-60 vol. %), olivine (15-20 vol. %), clinopyroxene (20-30 vol. %), amphibole (4-5 vol. %), chromite and Fe-Ti oxide minerals. Serpentine, chlorite and epidote are secondary phases (Fig. 4f). The olivine gabbronorite displays granular to poikilitic textures and is characterized by plagioclase (45-50 vol. %), clinopyroxene (25-30 vol. %), orthopyroxene (10-15 vol. %), amphibole (4-5 vol. %) and Fe-Ti oxides (Fig. 4g). The isotropic gabbros of the ophiolite in the region crop out in a very narrow area in the field and is represented by olivine gabbronorite. It displays a non-cumulus granular to poikilitic texture, and is represented by primary plagioclase (60-65 vol. %), clinopyroxene (30-35 vol. %), olivine (10-15 vol. %), orthopyroxene (7-8 vol. %) and Fe-Ti oxides (Fig. 4h). The rocks from the isotropic gabbro section include secondary alteration minerals such as calcite, chlorite, epidote and kaolinite.

4. GEOCHEMISTRY

4.1. Analytic techniques

A total of 9 samples from the mafic cumulates were analysed for major and trace elements by XRF in the laboratory of Earth Sciences Applications and Research Center (YEBİM) of Ankara University, Turkey. The major element contents were determined on glass beads fused from ignited powders to which $Li_2B_4O_7$ was added at a ratio 1:5, in a gold-platinum crucible at 1150 °C. The trace element contents were measured by XRF on pressed-powder pellets. The same samples were analysed by ICP-MS for trace elements (including REE) at Acme Analytical Laboratories in Canada. In the sample autoclave digestion, for each sample a 0.2 g pulverized sample was weighted into a graphite crucible and mixed with 1.5 g of $LiBO_2$ flux in a muffle furnace for 15 minutes at 1050 °C. The molten mixture was removed and quickly poured into 100 ml of 5% HNO_3 (ACS-grade nitric acid in demineralized water). The solution were shaken for two hours and then aliquot was poured into a polypropylene test tube. Standards and reagent blanks were added to the sample sequence. At the second stage, sample solutions were aspirated into an ICP mass spectrometer (Perkin-Elmer Elan 6000) or an ICP emission spectrometer (Jarrel Ash Atomcomp Model 975) for determination of element content. A total of representati-

ve 3 polished thin sections of the ophiolitic rocks were used to conduct electron microprobe analysis using a JEOL JXA-8600 in the Department of Lithospheric Research at Vienna University, Austria. The analytical conditions for the elements were 13 s (10 s for Peak and 3 s for Background) of counting interval, beam current was -20 nA and acceleration voltage was -15 kV.

4.2. Whole rock Chemistry

Major-trace and Rare Earth Elements (REE) analyses for the mafic cumulates from the southern part of Kahramanmaraş are given in Tables 1-2. Loss on ignition (LOI) values vary between 2,5 % and 5,47 % in cumulate gabbros. The different LOI values is because of variable secondary alteration which is indicated by the presence of mineral phases such as serpentine group minerals, epidote, calcite and chlorite.

The rock samples from the cumulate gabbros are plotted in the subalkaline field in total alkali-silica diagram of Irivine and Baragar, 1971 (Fig. 5). TiO_2 vs Mafic Index (FeO_t/FeO_t+MgO) diagram of Serri, 1980 separates High-Ti ophiolites and Low-Ti ophiolites (Fig. 6). The mafic cumulate rocks (except one sample) are plotted in the Low-Ti ophiolite field in this diagram (Fig. 6). Fig. 7a presents N-MORB-normalized spider diagrams of the mafic cumulate rocks from the Kahramanmaraş region. The spider pattern of the IAT-type Isotropic gabbroic rocks from Kızıldağ ophiolite (Bağcı et al., 2008) is plotted in this figure for comparation. The samples show some selected Large Ion Lithophile (LIL) element enrichment (Rb, Ba, Th, K) and Nb depletion, and flat patterns of high field strength (HFS) elements relative to N-MORB (Fig. 7a). The samples also show highly depleted Ti patterns. Th enrichment and Nb depletion are features of the mafic rocks formed in the subduction-related environment (Wood et al., 1979; Pearce, 1983; Arculus and Powel, 1986; Yogodzinski et al., 1993; Wallin and Metcalf, 1998). The Th enrichment and Nb depletion in the mafic rocks indicate their forma-

Table 1. **Major and trace element contents of the ophiolitic rocks**

Sample	Olivine gabbronorite				Olivine gabbro				Gabbro
	MT-2	MT-3	MT-4	MT-5	MT-27	MT-48	MT-50	MT-9	MT-14
SiO_2	46.61	46.07	45.46	46.71	49.10	46.53	49.41	45.89	45.28
TiO_2	0.14	0.16	0.15	0.12	0.13	0.10	0.21	0.15	0.04
Al_2O_3	17.07	15.04	16.86	17.99	12.30	19.37	11.40	14.06	17.93
FeO*	6.21	6.59	6.01	4.65	7.60	4.51	5.14	16.81	10.67
MnO	0.10	0.11	0.10	0.08	0.13	0.08	0.11	0.26	0.17
MgO	11.79	12.84	11.37	9.56	14.94	9.06	13.13	9.95	7.97
CaO	15.27	15.02	15.37	16.91	12.28	16.62	17.15	8.76	12.09
Na_2O	0.09	0.09	0.08	0.09	0.08	0.08	0.09	0.10	0.09
K_2O	0.11	0.10	0.11	0.10	0.11	0.13	0.07	0.24	0.09
P_2O_5	0.00	0.01	0.01	0.01	0.01	0.00	0.00	0.00	0.01
Cr_2O_3	0.09	0.12	0.15	0.09	0.16	0.04	0.23	0.00	0.02
LOI	1.95	3.12	3.62	3.02	2.54	2.87	2.41	3.23	4.87
Total	99.41	99.26	99.29	99.33	99.39	99.40	99.35	99.46	99.24
Nb	3.4	2.9	3.4	3.3	3.4	2.9	2.6	4.1	3.4
Zr	11.5	4.3	4.9	4.1	7.2	6.6	5.2	5.5	4.8
Y	4.3	4.6	4.9	4.1	3.4	2.8	5.4	1.6	1.3
Sr	69	57.7	73.7	72.3	25.9	66.7	58.1	64.2	33
U	20.8	8.7	9.2	9.3	9.6	9.9	9.1	8.8	9.3
Rb	0.4	0.7	0.4	0.3	0.5	0.3	0.3	3.7	0.6
Th	1	1	1	0.9	1.1	0.8	0.9	2.1	1.3
Pb	1	0.4	bdl	0.6	bdl	bdl	bdl	bdl	bdl
Ga	11.9	9.3	12.6	12	8.4	12.6	9.5	12.5	15.5
Ni	225	278.1	294.7	209.2	381.9	119.8	260.1	147.4	70.6
Co	70.6	58.6	50	47.5	74	42.9	35	82.2	63.6
Ce	14.9	10	17.6	13.7	11	10	19.8	11	19.1
Ba	5.4	10.8	14.9	5.4	26.9	5.3	5.5	39	10
Cs	5.4	6.2	3.6	5.6	bdl	4.4	5.9	bdl	bdl
La	9	7.5	18.8	9.4	7.8	7.6	12.6	10.5	11.6
Hf	bdl	bdl	8.7	bdl	7.2	bdl	5.6	bdl	5
Nb/Y	0.79	0.63	0.69	0.80	1.00	1.04	0.48	2.56	2.62

Total Fe is expressed as FeO*. LOI, Lost on ignition.

Table 2. **Trace element and REE compositions of the samples analysed by ICP-MS**

Sample	Olivine gabbronorite		Olivine gabbro					Gabbro	
	MT-2	MT-3	MT-4	MT-5	MT-27	MT-48	MT-50	MT-9	MT-14
W	152.7	115.5	76.9	114.4	186.9	104.6	45.0	87.6	65.3
Ba	3	6	6	2	19	3	6	34	5
Co	47.9	48.9	45.7	36.4	55.1	35.6	31.1	78.5	53.4
Ga	9.5	9.2	9.5	9.1	7.0	10.1	7.7	11.6	11.3
Hf	<0.1	<0.1	0.1	<0.1	<0.1	<0.1	0.3	<0.1	<0.1
Nb	1.1	0.9	1.0	0.8	<0.1	<0.1	<0.1	0.2	0.1
Rb	0.2	0.3	0.4	0.1	0.2	0.1	0.1	2.6	0.5
Sr	75.2	62.9	77.9	72.9	27.2	68.5	58.6	67.1	35.3
Ta	0.1	<0.1	<0.1	<0.1	<0.1	<0.1	<0.1	<0.1	<0.1
Th	<0.2	<0.2	<0.2	<0.2	<0.2	<0.2	<0.2	<0.2	<0.2
U	<0.1	<0.1	<0.1	<0.1	<0.1	<0.1	<0.1	<0.1	<0.1
V	132	158	153	127	138	126	193	608	152
Zr	2.2	2.8	4.3	1.9	3.1	1.3	4.6	1.2	0.9
Y	3.9	5.1	4.6	3.7	3.3	3.4	6.0	1.6	1.3
La	0.2	0.4	0.4	<0.1	0.4	0.4	0.4	0.1	<0.1
Ce	0.4	0.5	1.1	0.2	0.3	0.2	1.2	<0.1	<0.1
Pr	0.07	0.09	0.13	0.04	0.13	0.02	0.17	<0.02	<0.02
Nd	0.4	0.5	1.0	0.8	0.7	<0.3	1.3	<0.3	<0.3
Sm	0.29	0.33	0.38	0.23	0.21	0.14	0.44	<0.05	<0.05
Eu	0.17	0.19	0.19	0.16	0.09	0.13	0.22	<0.02	0.03
Gd	0.51	0.69	0.69	0.54	0.37	0.36	0.77	0.09	0.10
Tb	0.09	0.12	0.12	0.08	0.07	0.06	0.14	<0.01	<0.01
Dy	0.69	0.83	0.84	0.78	0.70	0.64	1.06	0.19	0.18
Ho	0.17	0.19	0.20	0.15	0.13	0.12	0.23	0.07	0.03
Er	0.48	0.52	0.51	0.40	0.43	0.41	0.66	0.22	0.22
Tm	0.07	0.08	0.07	0.05	0.06	0.03	0.09	0.03	0.03
Yb	0.57	0.50	0.43	0.37	0.38	0.36	0.60	0.42	0.27
Lu	0.05	0.06	0.06	0.05	0.05	0.04	0.08	0.04	0.04

tion in a subduction-related tectonic setting. The chondrite normalized rare earth element diagram for the mafic cumulate rocks from the Kahramanmaraş region is presented in Fig. 7b. The REE element patterns of the olivine gabbronorite and olivine gabbros exhibit generally flat to slight light rare earth element (LREE) depleted patterns with respect to heavy rare earth element (HREE), whereas the gabbros show generally REE depleted patterns relative to other samples. These samples exhibit a slight Eu negative anomaly (Fig. 7b), as a result of the removal of feldspar by the process of fractional crystallization or the partial melting of a source material in which feldspar is retained in the source (Rollinson 1993). In general, variation and depletion of REE patterns in the gabbroic cumulates may be attributed to high amount of cumulus phases (plagioclase, pyroxene and olivine) and small amount of intercumulus melt. Also, the flat HREE patterns shown by most these rocks are consistent with the presence of significant amounts of clinopyroxene (Berger et al., 2001). The general trend of the spider diagram show close similarities with the IAT-type isotropic gabbros from the Kızıldağ ophiolite (Figure 7a). On the other hand, the REE plots of the studied rocks are seen as more depleted than the isotropic gabbros from the Kızılağ ophiolite (Figure 7b).

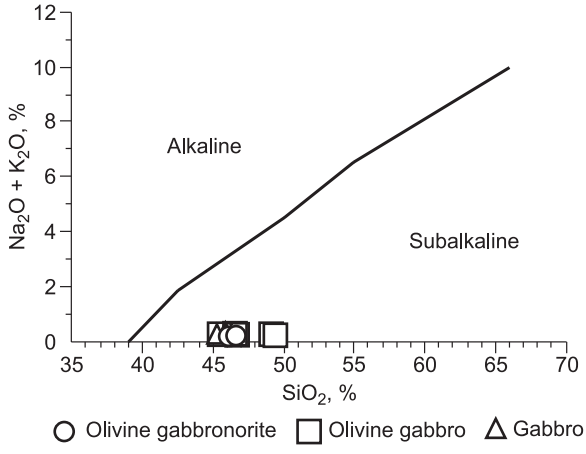

Fig. 5. Total alkali-silica diagram for the mafic cumulates (Irvine and Baragar, 1971)

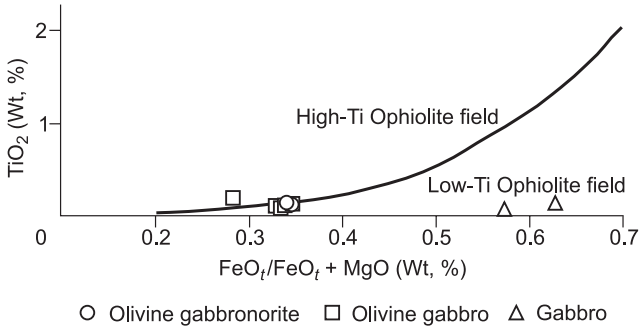

Fig. 6. TiO_2 vs Mafic index (FeOt/FeOt+MgO) diagrams for the cumulate gabbros (Serri, 1980)

The ophiolites formed in suprasubduction zone tectonic setting are divided into three different environments as island arc, back-arc and fore-arc basins according to the generation of the oceanic crust. On the other hand, they often show a geochemical stratigraphy including island arc tholeiites (IAT), and boninitic characters (Beccaluva et al., 1984; Malpas and Langdon, 1984; Beccaluva and Serri, 1988; Smellie et al., 1995; Bedard et al., 1998; Dilek and Flower, 2003; Beccaluva et al., 2004; Saccani and Photiades, 2004, 2005; Beccaluva et al., 2005; Bağcı and Parlak, 2009; Bağcı et al., 2006, 2008). In the tholeiitic magmas, flat to slightly LREE-depletion is a characteristic feature and there are a number of studies on the intra oceanic subduction zone type ophiolites of the eastern Mediterranean region showing the same characteristics (Alabaster et al., 1982; Parlak, 1996; Yalınız et al., 1996; Parlak et al., 2000; Al-Riyami et al., 2002; Beccaluva et al., 2004, 2005; Saccani and Photiades, 2005; Rızaoğlu et al., 2006; Pe-Piper et al., 2004; Meffre et al., 1996, Bağcı and Parlak, 2009). If the spider and REE diagrams are interpreted together, it is clearly seen that, the samples show IAT-type magma characteristics.

4.3. Mineral chemistry

Mineral chemistry analyses were performed on a total of 302 points on three representative samples (gabbro, olivine gabbro and olivine gabbronorite) from the mafic cumulate phase of the ophiolitic rocks from the southern part of Kahramanmaraş city (Tables 3-7)

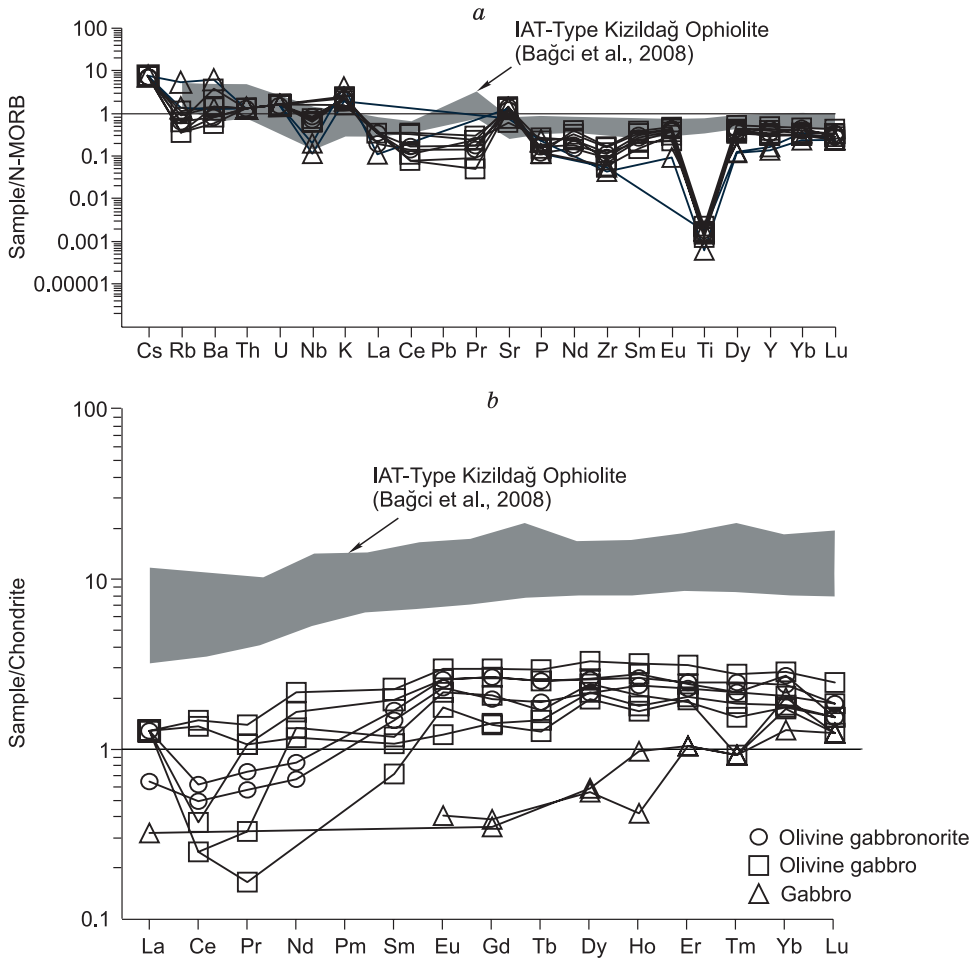

Fig. 7. (*a*) Spider diagrams (normalizing values are from Sun & McDonough, 1989) and (*b*) REE diagrams (normalizing values are from Boynton, 1984) for the mafic rocks

Table 3. **Representative analyses of major elements for olivines in the mafic cumulate rocks**

Sample	Olivine gabbronorite								Olivine gabbro							
	9MT2	11MT2	14MT2	79MT2	81MT2	110MT2	111MT2	115MT2	248MT48	249MT48	279MT48	310MT48	311MT48	312MT48	313MT48	314MT48
SiO_2	38.57	38.29	38.57	38.76	38.72	38.63	38.33	38.76	39.19	39.11	38.98	39.52	39.32	39.33	39.21	39.26
TiO_2	0.00	0.00	0.00	0.00	0.00	0.00	0.00	0.00	0.00	0.00	0.00	0.00	0.00	0.00	0.00	0.00
M_2O_3	0.01	0.00	0.00	0.00	0.00	0.00	0.00	0.01	0.00	0.00	0.00	0.00	0.00	0.00	0.00	0.00
Cr_2O_3	0.00	0.02	0.00	0.00	0.01	0.02	0.00	0.00	0.00	0.00	0.03	0.00	0.01	0.01	0.00	0.00
FeO*	20.25	20.10	19.59	20.10	19.89	20.18	19.88	20.09	17.51	17.72	17.59	17.07	17.33	17.08	17.16	17.27
MnO	0.30	0.31	0.28	0.33	0.31	0.31	0.27	0.26	0.27	0.29	0.30	0.28	0.30	0.30	0.29	0.27
MgO	40.85	40.84	40.96	41.17	40.97	40.71	40.68	40.61	42.80	42.97	42.95	43.30	43.09	43.24	43.25	43.09
NiO	0.17	0.13	0.13	0.16	0.13	0.11	0.18	0.14	0.08	0.12	0.14	0.10	0.10	0.13	0.12	0.12
CaO	0.09	0.07	0.04	0.06	0.07	0.07	0.07	0.04	0.21	0.19	0.04	0.06	0.05	0.06	0.05	0.08
Total	100.23	99.76	99.56	100.57	100.10	100.02	99.40	99.91	100.05	100.40	100.01	100.32	100.19	100.15	100.07	100.08
Si	0.99	0.99	1.00	0.99	1.00	1.00	0.99	1.00	1.00	0.99	0.99	1.00	1.00	1.00	1.00	1.00
Ti	0.00	0.00	0.00	0.00	0.00	0.00	0.00	0.00	0.00	0.00	0.00	0.00	0.00	0.00	0.00	0.00
Al	0.00	0.00	0.00	0.00	0.00	0.00	0.00	0.00	0.00	0.00	0.00	0.00	0.00	0.00	0.00	0.00
Cr	0.00	0.00	0.00	0.00	0.00	0.00	0.00	0.00	0.00	0.00	0.00	0.00	0.00	0.00	0.00	0.00
Fe	0.44	0.43	0.42	0.43	0.43	0.43	0.43	0.43	0.37	0.38	0.37	0.36	0.37	0.36	0.36	0.37
Mn	0.01	0.01	0.01	0.01	0.01	0.01	0.01	0.01	0.01	0.01	0.01	0.01	0.01	0.01	0.01	0.01
Mg	1.57	1.57	1.58	1.57	1.57	1.56	1.57	1.56	1.62	1.63	1.63	1.63	1.63	1.63	1.64	1.63
Ni	0.00	0.00	0.00	0.00	0.00	0.00	0.00	0.00	0.00	0.00	0.00	0.00	0.00	0.00	0.00	0.00
Ca	0.00	0.00	0.00	0.00	0.00	0.00	0.00	0.00	0.01	0.01	0.00	0.00	0.00	0.00	0.00	0.00
Total	3.01	3.01	3.00	3.01	3.00	3.00	3.01	3.00	3.00	3.01	3.01	3.00	3.00	3.00	3.00	3.00
Fo	78.24	78.37	78.85	78.50	78.60	78.24	78.49	78.29	81.34	81.21	81.32	81.89	81.60	81.86	81.80	81.64
Fa	21.76	21.63	21.15	21.50	21.40	21.76	21.51	21.71	18.66	18.79	18.68	18.11	18.40	18.14	18.20	18.36

Number of ions on the basis of 4 (O). Total Fe is expressed as FeO*.

Table 4. **Representative analyses of major elements for clinopyroxenes in the mafic cumulate rocks**

Sample			Olivine gabbronorite					Gabbro					Olivine gabbro			
	5MT2	50MT2	64MT2	70MT2	121MT2	133MT2	208MT14	209MT14	210MT14	211MT14	237MT48	239MT48	267MT48	268MT48	300MT48	303MT48
SiO_2	51.78	52.13	52.46	53.45	52.18	52.06	51.24	51.36	51.37	51.78	52.20	52.42	53.37	52.52	52.83	52.80
Al_2O_3	2.17	1.97	1.55	0.59	2.59	2.16	1.72	2.10	2.06	1.94	2.08	2.06	1.81	2.04	1.94	2.19
TiO_2	0.46	0.43	0.24	0.20	0.31	0.33	0.15	0.15	0.10	0.13	0.37	0.28	0.22	0.23	0.21	0.23
FeO*	5.98	5.95	5.03	4.40	6.00	5.97	10.13	8.38	8.11	8.80	5.25	5.16	6.36	5.19	5.57	5.47
MnO	0.19	0.16	0.15	0.18	0.18	0.17	0.24	0.20	0.22	0.21	0.22	0.17	0.15	0.15	0.16	0.15
MgO	16.99	16.73	16.34	16.79	16.27	16.63	14.22	14.78	14.83	15.06	16.62	17.51	18.86	17.27	17.88	17.69
Cr_2O_3	0.24	0.31	0.23	0.17	0.30	0.24	0.02	0.02	0.02	0.00	0.02	0.03	0.11	0.15	0.13	0.17
CaO	21.33	21.84	23.23	23.87	21.66	21.50	21.30	22.15	22.15	21.61	21.85	20.66	18.73	21.66	20.81	21.08
Na_2O	0.23	0.21	0.20	0.17	0.27	0.23	0.12	0.08	0.07	0.07	0.16	0.07	0.11	0.13	0.15	0.13
K_2O	0.00	0.01	0.01	0.00	0.01	0.00	0.00	0.02	0.01	0.02	0.02	0.00	0.00	0.02	0.00	0.00
Total	99.36	99.73	99.44	99.82	99.76	99.30	99.13	99.23	98.94	99.61	98.79	98.36	99.71	99.34	99.67	99.92
Si	1.92	1.93	1.94	1.97	1.92	1.93	1.94	1.93	1.93	1.94	1.94	1.95	1.95	1.94	1.94	1.93
Al (IV)	0.08	0.07	0.06	0.03	0.08	0.07	0.06	0.07	0.07	0.06	0.06	0.05	0.05	0.06	0.06	0.07
Al (VI)	0.01	0.01	0.01	0.00	0.04	0.02	0.02	0.02	0.02	0.02	0.03	0.04	0.03	0.02	0.02	0.03
Ti	0.01	0.01	0.01	0.01	0.01	0.01	0.00	0.00	0.00	0.00	0.01	0.01	0.01	0.01	0.01	0.01
Fe^{3+}	0.01	0.01	0.01	0.01	0.01	0.01	0.02	0.01	0.01	0.01	0.01	0.01	0.01	0.01	0.01	0.01
Fe^{2+}	0.18	0.17	0.15	0.13	0.18	0.18	0.30	0.25	0.24	0.26	0.15	0.15	0.18	0.15	0.16	0.16
Mn	0.01	0.01	0.00	0.01	0.01	0.01	0.01	0.01	0.01	0.01	0.01	0.01	0.00	0.00	0.00	0.00
Mg	0.94	0.92	0.90	0.92	0.89	0.92	0.80	0.83	0.83	0.84	0.92	0.97	1.03	0.95	0.98	0.97
Cr	0.01	0.01	0.01	0.00	0.01	0.01	0.00	0.00	0.00	0.00	0.00	0.00	0.00	0.00	0.00	0.00
Ca	0.85	0.86	0.92	0.94	0.86	0.85	0.86	0.89	0.89	0.87	0.87	0.82	0.73	0.86	0.82	0.83
Na	0.02	0.02	0.01	0.01	0.02	0.02	0.01	0.01	0.00	0.00	0.01	0.01	0.01	0.01	0.01	0.01
K	0.00	0.00	0.00	0.00	0.00	0.00	0.00	0.00	0.00	0.00	0.00	0.00	0.00	0.00	0.00	0.00
Total	4.03	4.02	4.02	4.02	4.01	4.02	4.02	4.02	4.02	4.02	4.01	4.00	4.01	4.02	4.02	4.01
Ens	47.49	46.65	45.46	45.98	46.10	46.81	40.24	41.62	41.87	42.25	46.96	49.53	52.44	48.21	49.60	49.15
Fs	9.67	9.57	8.09	7.04	9.83	9.70	16.46	13.56	13.19	14.18	8.68	8.46	10.14	8.35	8.92	8.76
Wo	42.84	43.78	46.45	46.98	44.08	43.50	43.30	44.83	44.94	43.57	44.37	42.01	37.42	43.44	41.48	42.09
Mg#	83.51	83.36	85.26	87.18	82.86	83.25	71.46	75.86	76.53	75.32	84.94	85.82	84.10	85.58	85.11	85.21

Number of ions on the basis of 6 (O). Total Fe is expressed as FeO*.

4.3.1. Olivine

The cumulus olivine analyses of the gabbroic cumulate rocks are presented in Table 3. The olivine minerals in mafic cumulates are represented by low SiO_2 (39.52-38.29%) and FeO (20.25-17.07 %), Cr_2O_3 (0.03-0 %), NiO (0.18-0.08 %), CaO (0.21-0.03 %) and high MgO (43.30-40.61 %) contents (Table 3). The Forsterite (Fo) contents of olivines range from 78.85 to 78.24 % in olivine gabbronorites and from 81.89 to 81.21 % in olivine gabbros (Table 3). According to the corelation of both mineral chemistry and microscopic studies, there is no visible zonation in the olivines.

Olivine compositions in mantle tectonites of the Eastern Mediterranean ophiolites (Kızıldağ-Hatay, Mersin, Pozantı-Karsantı etc.) vary between Fo_{92} and Fo_{89} and gradually decrease in cumulate gabbroic (Fo_{85-76}) rocks (Pişkin et al., 1990; Parlak et al., 1996, 2002), suggesting fractionation and differentiation of a similar parental magma (Spandler et al., 2003). The olivines from the studied gabbroic rocks display similar features of the cumulate gabbros of the Eastern Mediterranean ophiolites.

4.3.2. Clinopyroxene

The cumulus clinopyroxene analyses of the gabbroic cumulate rocks (olivine gabbronorite, gabbro and olivine gabbro) are presented in Table 4. The magnesium number [$Mg^{\#}$=(100*Mg/Mg+Fe)] of the cumulate rocks range from 76.53 to 71.46 in gabrros, from 85.82 to 84.10 in olivine gabbros, and from 87.18 to 82.16 in olivine gabbronorites (Table 4). The Wollastonite (Wo), Enstatite (Ens) and Ferrosillite (Frs) contents for gabbros, olivine gabbros and olivine gabbronorites are [$Wo_{44.94-43.30}$, $Ens_{42.25-40.24}$, $Frs_{16.46-13.19}$], [$Wo_{44.37-37.42}$, $Ens_{52.44-46.96}$, $Frs_{10.14-8.35}$], [$Wo_{46.98-42.84}$, $Ens_{47.49-45.46}$, $Frs_{9.83-7.04}$] respectively (Table 4). The compositions of clinopyroxenes are plotted in the field of diopside and show close similarities with the clinopyroxenes from the island arc setting in Fig. 8. Elthon (1987) stated that the clinopyroxenes with high TiO_2 and Cr_2O_3 contents also have high

Table 5. **Representative analyses of major elements for orthopyroxenes in the mafic cumulate rocks**

Sample	Olivine gabbronorite							Gabbro						
	123MT2	127MT2	128MT2	129MT2	130MT2	134MT2	137MT2	174MT14	176MT14	178MT14	212MT14	215MT14	229MT14	236MT14
SiO_2	54.76	54.79	54.63	54.64	54.75	54.85	54.27	53.07	52.08	52.38	52.27	52.09	52.01	51.59
Al_2O_3	1.40	1.33	1.26	1.26	1.40	1.22	1.44	1.11	1.00	1.04	1.16	1.20	1.04	1.01
TiO_2	0.27	0.22	0.21	0.22	0.21	0.21	0.21	0.04	0.05	0.06	0.05	0.05	0.05	0.07
FeO*	12.70	12.35	12.46	12.53	12.35	12.39	12.54	20.58	22.97	21.88	21.35	21.64	22.12	23.03
MnO	0.27	0.26	0.33	0.28	0.28	0.30	0.31	0.38	0.47	0.41	0.38	0.46	0.44	0.47
MgO	29.17	29.20	29.48	29.02	29.31	29.40	29.02	23.17	21.64	22.33	23.19	22.27	22.29	21.65
Cr_2O_3	0.10	0.17	0.10	0.16	0.13	0.11	0.13	0.05	0.02	0.04	0.03	0.02	0.03	0.06
CaO	1.23	1.56	1.17	1.62	1.44	1.21	1.62	1.40	1.34	1.36	0.94	1.56	0.98	1.13
Na_2O	0.00	0.00	0.00	0.02	0.01	0.00	0.03	0.00	0.00	0.00	0.00	0.01	0.00	0.00
K_2O	0.00	0.00	0.00	0.00	0.00	0.00	0.00	0.01	0.00	0.01	0.00	0.00	0.00	0.00
Total	99.90	99.87	99.65	99.74	99.87	99.69	99.57	99.80	99.58	99.50	99.38	99.30	98.96	99.01
Si	1.95	1.95	1.95	1.95	1.95	1.96	1.95	1.97	1.96	1.96	1.95	1.96	1.96	1.96
Al (IV)	0.05	0.05	0.05	0.05	0.05	0.04	0.05	0.03	0.04	0.04	0.05	0.04	0.04	0.04
Al (VI)	0.01	0.01	0.01	0.01	0.01	0.01	0.01	0.02	0.00	0.01	0.01	0.01	0.01	0.00
Ti	0.01	0.01	0.01	0.01	0.01	0.01	0.01	0.00	0.00	0.00	0.00	0.00	0.00	0.00
Fe^{3+}	0.02	0.02	0.02	0.02	0.02	0.02	0.02	0.03	0.04	0.03	0.03	0.03	0.03	0.04
Fe^{2+}	0.36	0.35	0.35	0.36	0.35	0.35	0.36	0.61	0.69	0.65	0.63	0.65	0.66	0.69
Mn	0.01	0.01	0.01	0.01	0.01	0.01	0.01	0.01	0.01	0.01	0.01	0.01	0.01	0.02
Mg	1.55	1.55	1.57	1.55	1.56	1.56	1.55	1.28	1.21	1.25	1.29	1.25	1.25	1.22
Cr	0.00	0.00	0.00	0.00	0.00	0.00	0.00	0.00	0.00	0.00	0.00	0.00	0.00	0.00
Ca	0.05	0.06	0.04	0.06	0.05	0.05	0.06	0.06	0.05	0.05	0.04	0.06	0.04	0.05
Total	4.01	4.01	4.01	4.01	4.01	4.01	4.02	4.01	4.01	4.01	4.02	4.02	4.01	4.02
Ens	78. 14	78. 09	78. 62	77. 65	78. 30	78. 63	77. 61	64. 47	60. 52	62. 36	64. 31	62. 22	62. 52	60. 73
Fs	19.50	18.92	19.14	19.23	18.94	19.05	19.28	32.72	36.78	34.91	33.82	34.64	35.51	36.99
Wo	2.37	3.00	2.24	3.12	2.76	2.32	3.11	2.80	2.70	2.74	1.88	3.13	1.97	2.28
Mg#	80.37	80.83	80.83	80.50	80.88	80.87	80.49	66.74	62.68	64.54	65.94	64.72	64.24	62.63

Number of ions on the basis of 6 (O). Total Fe is expressed as FeO*.

Table 6. **Representative analyses of major elements for plagioclases in the mafic cumulate rocks**

Sample	Olivine gabbronorite				Gabbro								Olivine gabbro			
	16MT2	56MT2	62MT2	146MT2	150MT14	153MT14	155MT14	187MT14	217MT14	219MT14	222MT14	223MT14	259MT48	288MT48	292MT48	297MT48
SiO_2	47.27	45.77	45.03	46.00	42.95	43.43	43.79	43.52	43.25	43.36	43.02	43.55	44.99	45.38	45.21	45.01
Al_2O_3	33.93	34.40	34.12	34.23	35.72	36.03	35.38	35.41	36.06	35.72	35.63	35.51	33.80	34.34	34.17	33.90
TiO_2	0.00	0.02	0.02	0.01	0.05	0.00	0.01	0.00	0.00	0.03	0.00	0.00	0.00	0.00	0.02	0.01
FeO*	0.42	0.43	0.45	0.45	0.62	0.51	0.54	0.51	0.59	0.59	0.54	0.449	0.393	0.533	0.514	0.49
MnO	0.00	0.04	0.00	0.00	0.01	0.00	0.00	0.00	0.00	0.01	0.04	0.02	0.00	0.00	0.01	0.00
MgO	0.01	0.03	0.01	0.01	0.02	0.03	0.01	0.00	0.01	0.00	0.00	0.01	0.04	0.09	0.06	0.11
CaO	16.82	18.18	18.23	17.85	19.83	19.90	19.78	19.82	19.86	19.87	19.76	19.49	17.98	18.22	18.23	18.24
Na_2O	2.05	1.41	1.28	1.39	0.29	0.34	0.43	0.34	0.32	0.36	0.35	0.43	1.30	1.21	1.11	1.05
K_2O	0.01	0.00	0.00	0.02	0.00	0.00	0.00	0.01	0.01	0.00	0.02	0.04	0.03	0.02	0.01	0.03
Total	100.51	100.27	99.15	99.96	99.49	100.22	99.93	99.60	100.09	99.94	99.36	99.50	98.54	99.79	99.33	98.83
Si	2.16	2.11	2.10	2.12	2.01	2.01	2.03	2.03	2.01	2.02	2.01	2.03	2.11	2.10	2.10	2.11
Al (IV)	0.84	0.90	0.91	0.88	1.00	1.00	0.97	0.98	1.00	0.99	1.00	0.98	0.90	0.91	0.90	0.90
Al (VI)	0.98	0.96	0.96	0.98	0.96	0.96	0.96	0.96	0.96	0.96	0.96	0.97	0.96	0.96	0.97	0.96
Ti	0.00	0.00	0.00	0.00	0.00	0.00	0.00	0.00	0.00	0.00	0.00	0.00	0.00	0.00	0.00	0.00
Fe	0.02	0.02	0.02	0.02	0.02	0.02	0.02	0.02	0.02	0.02	0.02	0.02	0.02	0.02	0.02	0.02
Mn	0.00	0.00	0.00	0.00	0.00	0.00	0.00	0.00	0.00	0.00	0.00	0.00	0.00	0.00	0.00	0.00
Mg	0.00	0.00	0.00	0.00	0.00	0.00	0.00	0.00	0.00	0.00	0.00	0.00	0.00	0.01	0.00	0.01
Ca	0.82	0.90	0.91	0.88	0.99	0.99	0.98	0.99	0.99	0.99	0.99	0.97	0.90	0.90	0.91	0.91
Na	0.18	0.13	0.12	0.12	0.03	0.03	0.04	0.03	0.03	0.03	0.03	0.04	0.12	0.11	0.10	0.09
K	0.00	0.00	0.00	0.00	0.00	0.00	0.00	0.00	0.00	0.00	0.00	0.00	0.00	0.00	0.00	0.00
Total	5.00	5.00	5.00	5.00	5.00	5.00	5.00	5.00	5.00	5.00	5.00	5.00	5.00	5.00	5.00	5.00
Or	0.05	0.02	0.00	0.13	0.02	0.00	0.02	0.06	0.05	0.01	0.10	0.23	0.18	0.10	0.03	0.15
Ab	18.07	12.31	11.29	12.29	2.58	2.95	3.77	2.97	2.83	3.16	3.11	3.82	11.53	10.69	9.91	9.38
An	81.88	87.67	88.71	87.48	97.40	96.90	96.15	96.96	97.12	96.73	96.79	95.90	88.29	89.21	90.06	90.47

Number of ions on the basis of 16 (O). Total Fe is expressed as FeO*.

Table 7. **Representative analyses of major elements for amphiboles in the mafic cumulate rocks**

Sample	Olivine gabbronorite							Gabbro						Olivine gabbro
	22MT2	25MT2	26MT2	30MT2	32MT2	87MT2	90MT2	168MT14	181MT14	185MT14	196MT14	206MT14	230MT14	270MT48
SiO_2	45.24	50.04	51.26	49.64	52.76	44.52	52.04	55.14	54.58	51.50	53.88	50.45	49.69	54.42
TiO_2	1.64	0.35	0.28	0.26	0.15	1.54	0.20	0.02	0.04	0.11	0.07	0.20	0.30	0.12
Al_2O_3	10.16	8.20	6.54	7.91	5.02	10.44	4.20	0.84	0.79	5.77	0.96	4.78	6.36	2.53
C_r2O_3	0.63	0.22	0.59	0.06	0.00	0.59	0.04	0.03	0.01	0.08	0.02	0.01	0.03	0.05
FeO	8.57	6.65	6.41	7.50	6.24	8.19	6.15	19.62	19.59	10.55	20.47	13.22	11.64	6.20
MnO	0.12	0.13	0.12	0.19	0.15	0.11	0.15	0.40	0.44	0.19	0.46	0.20	0.14	0.17
MgO	16.20	18.37	18.69	18.22	19.63	16.65	19.88	20.61	20.65	17.42	19.21	15.62	16.45	20.55
CaO	12.00	12.88	12.74	12.32	12.78	12.16	12.82	0.62	0.73	10.96	1.39	11.31	11.32	12.32
Na_2O	1.91	1.07	0.99	1.52	0.85	2.30	0.96	0.02	0.05	0.69	0.07	0.45	0.75	0.43
K_2O	0.23	0.00	0.01	0.01	0.00	0.23	0.00	0.02	0.00	0.03	0.01	0.14	0.08	0.02
Total	96.68	97.91	97.63	97.61	97.57	96.72	96.43	97.31	96.88	97.28	96.53	96.37	96.75	96.80
Si	6.51	6.98	7.17	6.95	7.34	6.42	7.35	7.93	7.88	7.17	7.87	7.23	7.04	7.57
Al (IV)	1.49	1.02	0.83	1.05	0.66	1.58	0.65	0.07	0.12	0.83	0.13	0.77	0.96	0.41
Al (VI)	0.23	0.33	0.24	0.26	0.17	0.19	0.05	0.07	0.02	0.12	0.03	0.03	0.10	0.00
Fe^{+3}	0.56	0.45	0.38	0.61	0.42	0.56	0.42	0.00	0.08	1.22	0.06	1.08	1.14	0.63
Ti	0.18	0.04	0.03	0.03	0.02	0.17	0.02	0.00	0.00	0.01	0.01	0.02	0.03	0.01
Cr	0.07	0.02	0.06	0.01	0.00	0.07	0.00	0.00	0.00	0.01	0.00	0.00	0.00	0.01
Fe^{+2}	0.47	0.32	0.37	0.27	0.31	0.43	0.31	2.36	2.29	0.00	2.44	0.51	0.23	0.09
Mn	0.01	0.02	0.01	0.02	0.02	0.01	0.02	0.05	0.05	0.02	0.06	0.02	0.02	0.02
Mg	3.47	3.82	3.90	3.80	4.07	3.58	4.18	4.42	4.45	3.61	4.18	3.34	3.47	4.26
Ca	1.85	1.92	1.91	1.85	1.91	1.88	1.94	0.10	0.11	1.63	0.22	1.73	1.72	1.84
Na	0.53	0.29	0.27	0.41	0.23	0.64	0.26	0.00	0.01	0.19	0.02	0.12	0.20	0.12
K	0.04	0.00	0.00	0.00	0.00	0.04	0.00	0.00	0.00	0.00	0.00	0.03	0.02	0.00
Total	15.42	15.21	15.18	15.26	15.14	15.56	15.20	15.00	15.01	14.82	15.02	14.88	14.94	14.96
Mg#	77.11	83.12	83.86	81.25	84.86	78.36	85.21	65.20	65.27	74.64	62.60	67.82	71.58	85.53

Number of ions is on the basis of 23 (O). Total Fe is expressed as FeO*

Al_2O_3, and this is the property for high pressure clinopyroxenes. The clinopyroxenes from the gabbroic cumulates are mostly plotted in the field of low pressure clinopyroxenes field in Fig. 9, and show close similarity with the clinopyroxenes from the cumulates of Pozantı-Karsantı ophiolite (Parlak et al., 2002), and Kömürhan ophiolite (Rızaoğlu, 2006). As a result of the clinopyroxene fractionation, the Cr contents of the mafic cumulates are

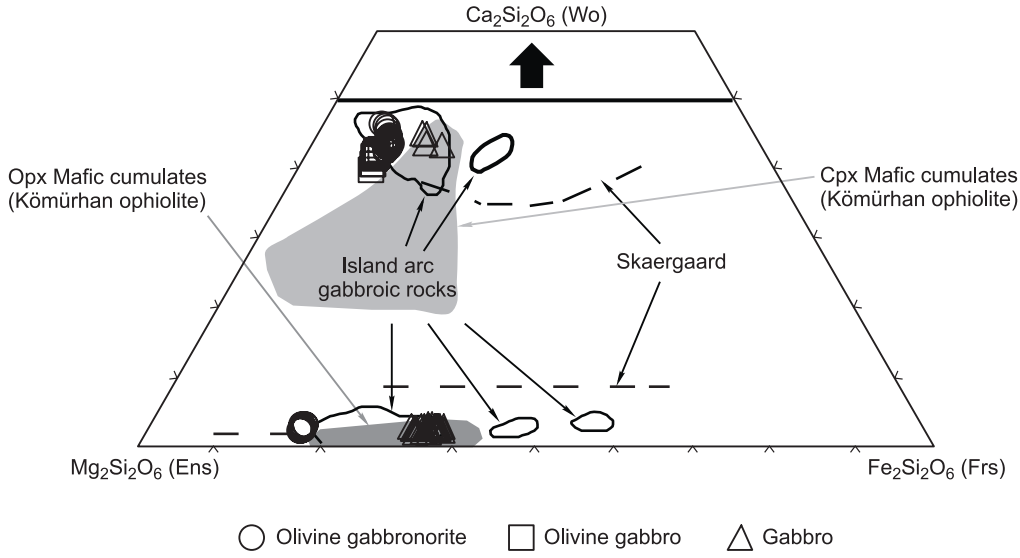

Fig. 8. Ortho and Clinopyroxene ternary diagram showing clinopyroxene and orthopyroxene compositions from the mafic cumulates of the ophiolites from southern Kahramanmaraş. Fields of the gabbroic rocks from the Kömürhan ophiolite are from Rızaoğlu, 2006. Fields of island-arc gabbroic rocks and Skaergaard trends are from Burns, 1985).

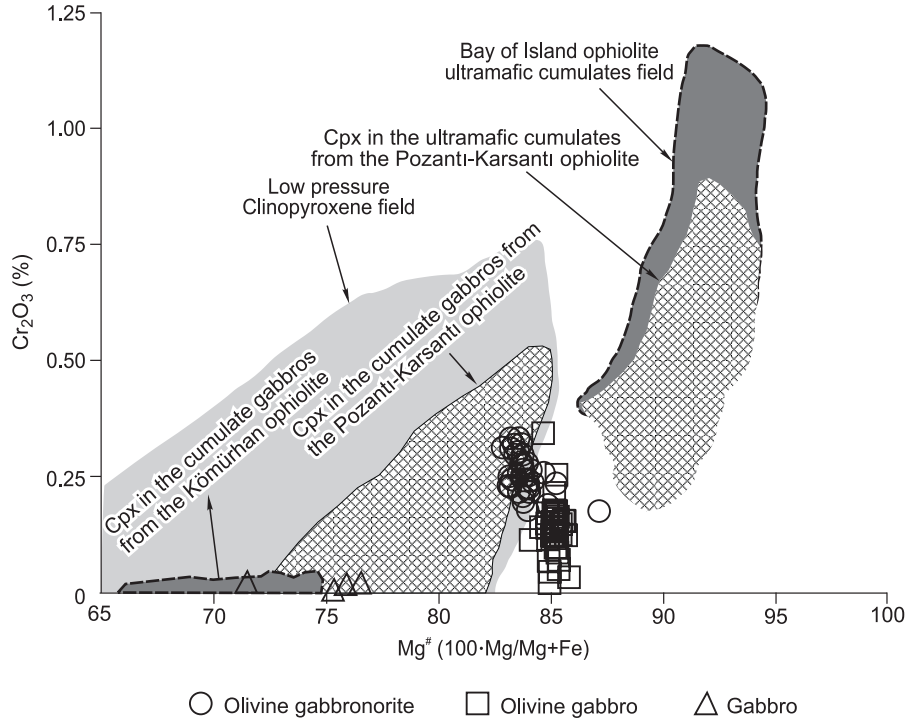

Fig. 9. Cr_2O_3 versus Mg number in clinopyroxenes of the ultramafic cumulates. Field of Bay Of Island ophiolite ultramafic cumulates is from Elthon et al., 1982, 1984. Low pressure clinopyroxene field is from Elthon, 1987. Field of clinopyroxenes in the mafic-ultramafic cumulates of the Pozantı-Karsantı Ophiolite is from Parlak et al., 2000. Field of clinopyroxenes in the mafic cumulates of the Kömürhan Ophiolite is from Rızaoğlu, 2006.

Fig. 10. Variation diagram of Ti versus Al^{IV} diagram for the clinopyroxenes from the ultramafic-mafic cumulates. Fields of MORB, IAT and boninite are from Beccaluva et al., 1989. Fields for the Pozantı-Karsantı ophiolite are from Parlak et al., 2000, 2002; Kömürhan ophiolite is from Rızaoğlu, 2006.

highly low (Table 4). Al^{IV} vs Ti contents variation diagram is shown in Fig. 10. The clinopyroxenes from the cumulates are plotted in IAT field and exhibit similar characteristics with the clinopyroxenes from the cumulates of Pozantı-Karsantı ophiolite (Parlak et al., 2002), and Kömürhan ophiolite (Rızaoğlu, 2006) (Fig. 10). The Mg numbers [$Mg^{\#}$=(100*Mg/Mg+Fe)] vs Al_2O_3 contents of the clinopyroxenes are plotted in Fig. 11. The clinopyroxenes from the gabbroic cumulates show close similarities with the mafic cumulates of Pozantı-Karsantı ophiolite (Parlak et al., 2002) and Tekirova (Antalya) ophiolite (Bağcı et al., 2008) and differ from the high pressure field defined by Medaris (1972).

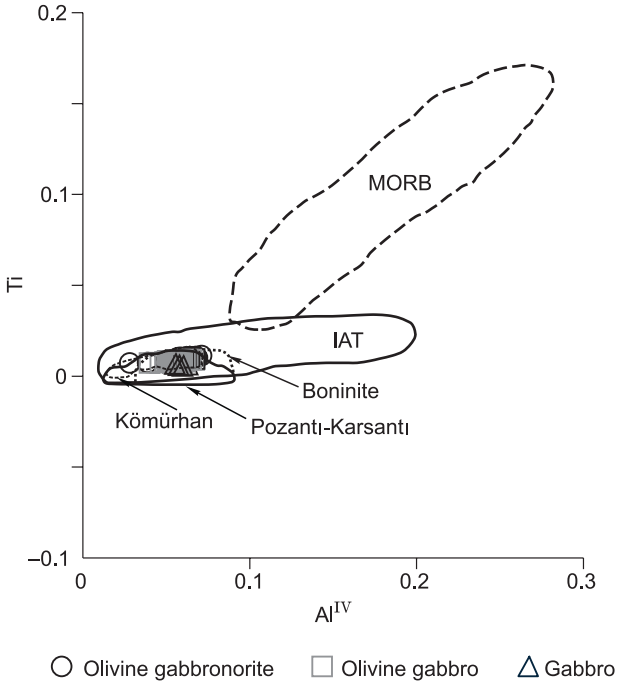

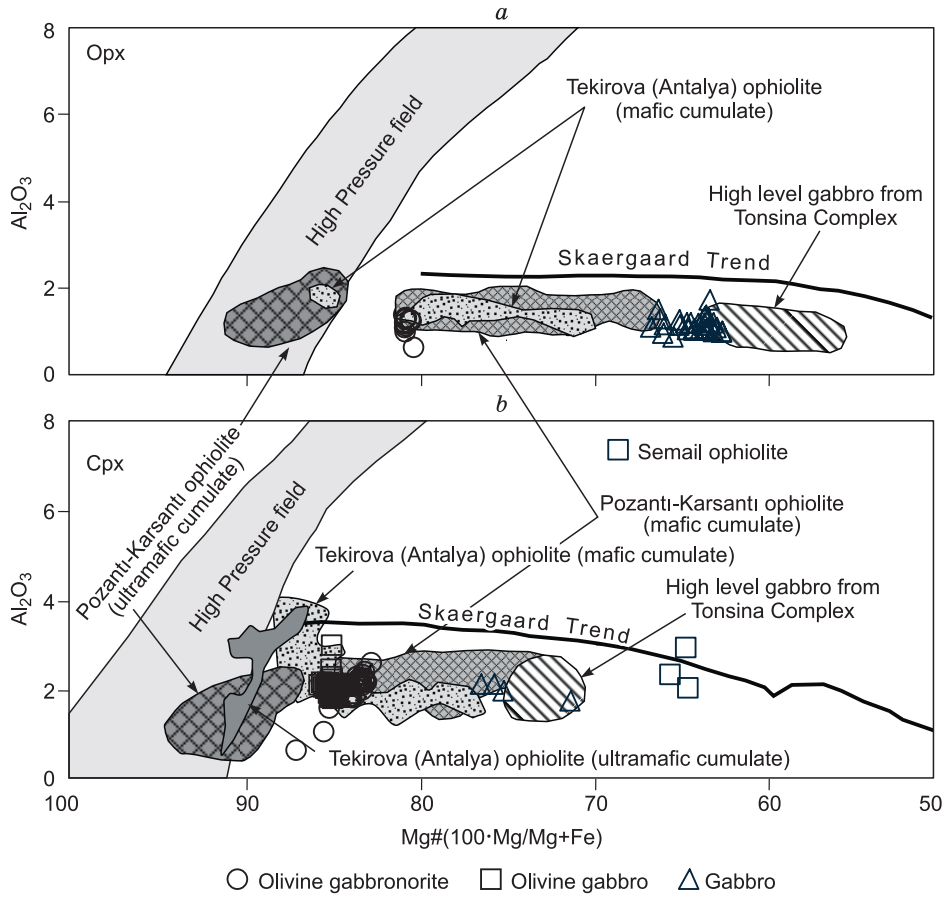

Fig. 11. Plot of Al_2O_3 versus Mg numbers in the orthopyroxenes (*a*) and clinopyroxenes (*b*) from the mafic cumulates of the ophiolitic rocks. The field of high-pressure peridotite is from Medaris, 1972; fields of Pozantı-Karsantı ophiolite are from Parlak et al., 2000; fields of Tekirova (Antalya) ophiolite are from Bağcı et al., 2006. The data of Skaergaard, Tonsina Complex, and Semail ophiolite are from DeBari and Coleman, 1989.

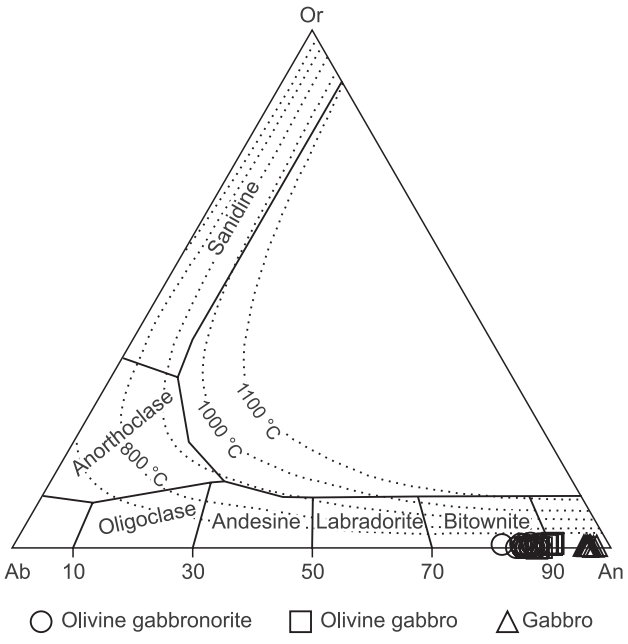

Fig. 12. Feldspar classification diagram (after Barth, 1962)

4.3.3. Orthopyroxene

Representative orthopyroxene analyses from the mafic cumulate rocks are presented in Table 5. The orthopyroxene composition is $Ens_{64.47\text{-}60.52,}$ $Frs_{36.99\text{-}32.72}$ $Wo_{3.13\text{-}1.88}$ in gabbros, and $Ens_{78.63\text{-}77.61,}$ $Frs_{19.50\text{-}18.92,}$ $Wo_{3.12\text{-}2.24}$ in olivine gabbronorites (Table 5). The Mg-numbers range from 66.74 to 62.63 in gabbros and from 80.88 to80.37 in olivine gabbronorites (Table 5). The compositions of orthopyroxenes are plotted in the field of hypersten and show close similarities with the orthopyroxenes from the island arc setting in Ens-Frs-Wo diagram of Burns, 1985 (Fig. 8). The high magnesium numbers [$Mg^{\#}$=(100*Mg/Mg+Fe)] of the orthopyroxenes show similar values with some Eastern Mediterranean ophiolites formed in an intraoceanic subduction zone such as Kızıldağ ophiolite (Bağcı, 2004; Bağcı et al., 2005), Pozantı-Karsantı Ophioite (Parlak et al., 2000, 2002), Mersin Ophiolite (Parlak, 1996; Parlak et al., 1996), Kömürhan ophiolite (Rızaoğlu et al., 2006), İspendere ophiolite (Parlak et al., 2012). In Mg numbers [$Mg^{\#}$=(100*Mg/Mg+Fe)] vs Al_2O_3 contents correlation diagram, the orthopyroxenes from the gabbroic cumu-

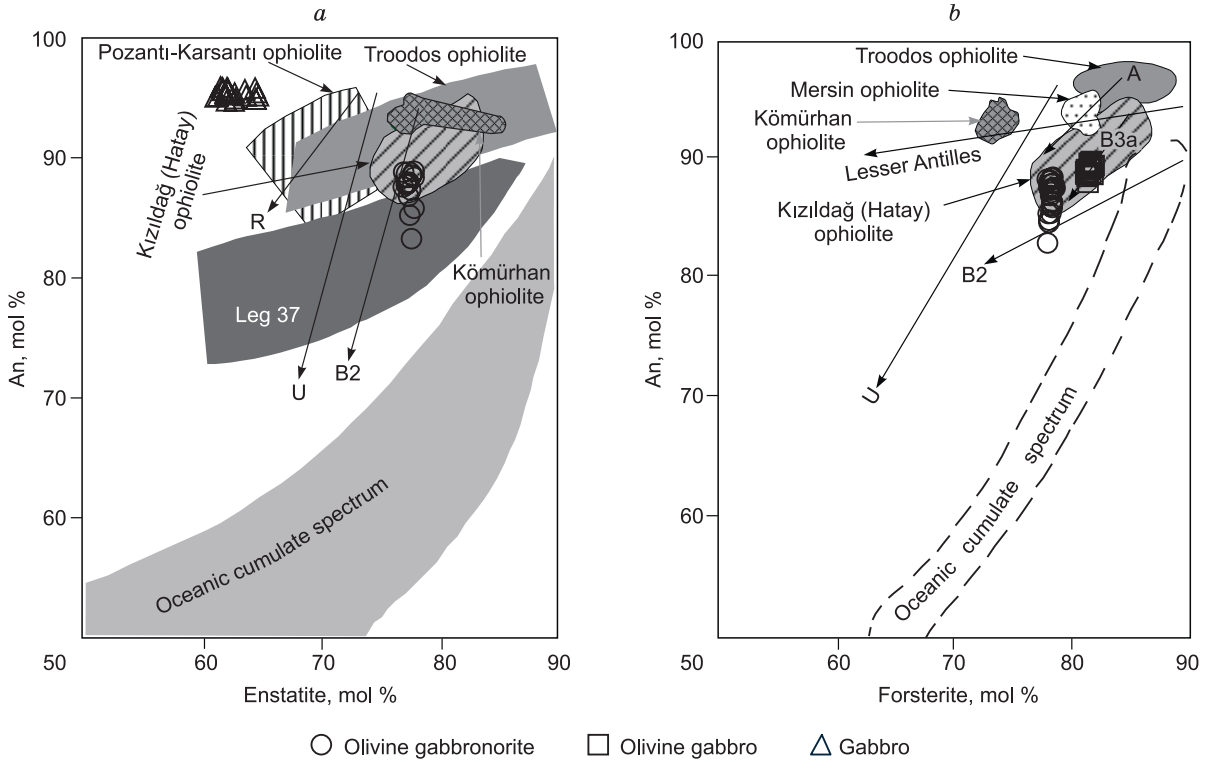

Fig. 13. (*a*) Anorthite content in plagioclase (mol %) versus enstatite content in orthopyroxene (mol %), (*b*) Anorthite content in plagioclase (mol %) versus Fo (mol %) content in olivine for the mafic cumulate rocks from the South of Kahramanmaraş. The Troodos ophiolite trend is from Hebert and Laurent, 1990. The Mersin ophiolite trend is from Parlak et al., 1996, The Pozantı-Karsantı ophiolite trend is from Parlak et al., 2000, The Kömürhan ophiolite field is from Rızaoğlu, 2006, Kızıldağ (Hatay) ophiolite field from Bağcı, 2004, R, Rindjami Volcano (Foden, 1983); B2, B3a, Boisa Volcano (Gust and Johnson, 1981); U, Usa Volcano (Fujimaki, 1986); A, Agrigan Volcano (Stern, 1979); Lesser Antilles is from Arculus and Wills, 1980.

lates show close similarities with the mafic cumulates of Pozantı-Karsantı ophiolite (Parlak et al., 2002) and Tekirova (Antalya) ophiolite (Bağcı et al., 2008) (Fig. 11).

4.3.4. Plagioclase

Representative plagioclase analyses from the mafic cumulate rocks (gabbro, olivine gabbro and olivine gabbronorite) are presented in Table 6. The plagioclases are unzoned. In the plagioclase classification diagram, all the rock samples are plotted in the bitownite and anorthite field (Fig. 12). The Anortite contents range from 97.40 to 96.15 % in gabbros, from 95.90 to 88.29 % in olivine gabbros and from 97.40 to 81.88 % in olivine gabbronorites (Table 6). Crystallization of such calcic-plagioclase is attributed to either high magmatic water contents (Arculus and Wills, 1980; Sisson and Grove, 1993; Panjasawatwong et al., 1997) or high melt Ca/(Ca+Na) ratios (Panjasawatwong et al., 1997).

Co-variations of An content of plagioclases versus Enstatite content of pyroxenes and Forsterite content of olivines from the cumulate gabbroic rocks (olivine gabbro and olivine gabbronorite) are plotted together with island arc settings and some eastern Mediterranean ophiolites [Troodos (Hébert and Laurent, 1990), Mersin (Parlak et al., 1996), Pozantı–Karsantı (Parlak et al., 2000) Kızıldağ (Bağcı et al., 2006), and Kömürhan (Rızaoğlu et al., 2006)] in Fig. 13. The cumulate gabbroic rocks differ from the MORB type gabbroic rocks and show close similarity to the gabbroic rocks from the subduction related environment. Co-variations of An content of plagioclases versus Mg numbers of clinopyroxenes diagram separates the gabbros formed in Mid Ocean Ridges (MOR) and arc environment (Fig. 14). The samples from this study are plotted together with some well-known Eastern Mediterranean ophiolites [Mersin and Pozantı-Karsantı (Parlak et al., 1996, 2000), Kızıldağ and Tekirova (Bağcı et al., 2005, 2006), The gabbros from the Kahramanmaraş region differ from MORB type gabbroic rocks and show close similarities to the gabbros from the well-known suprasubduction zone type ophiolites (Fig. 14).

4.3.5. Amphibole

Representative amphibole analyses from the mafic cumulate rocks (gabbro, olivine gabbro and olivine gabbronorite) are presented in Table 7. The amphiboles in the mafic cumulate rocks are secondary and they are derived from alteration of pyroxenes. They are represented by tremolite, actinolite, magnesio-hornblende and Tschermakite in the classification diagram of Leake et al. (1997) (Fig. 15). The Mg-numbers [$Mg^{\#}$=(100*Mg/Mg+Fe)] of the amphiboles are from 74.64 to 62.60 in gabbros, from 85.21 to 77.11 in olivine gabbronorites and 85.53 in olivine gabbro (Table 7).

5. DISCUSSION AND CONCLUSIONS

Unnamed ophiolitic rocks in the Kahramanmaraş region located between the Bitlis–Pütürge massif and the Arabian platform together with the Koçali, Hatay, and Baer-Bassit ophiolites that are adjacent with the Troodos ophiolite to the west. These ophiolites are well documented as formed by spreading above a north-dipping intra-oceanic subduction zone tectonic setting (Al-Riyami et al., 2002; Bağcı et al., 2005, 2008; Rızaoğlu et al., 2006; Parlak et al., 2009). These ophiolites were emplaced onto the Arabian continental margin during Campanian–Maastrichtian time (Inwood et al., 2009), and then were transgressively overlain by non-marine to shallow-marine sediments (Boulton et al., 2006; Boulton and Robertson, 2008). In supra-subduction zone (SSZ) settings, boninitic and tholeiitic magmas could occur (Yibas et al., 2003,

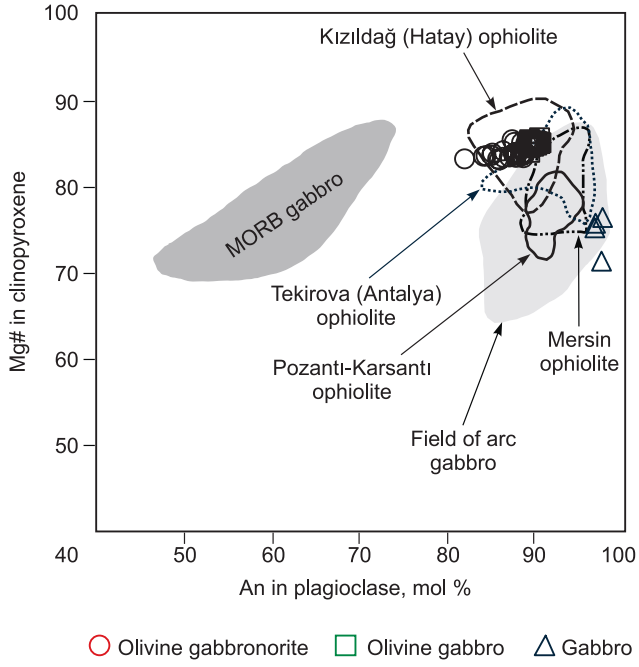

Fig. 14. Anorthite content in plagioclase (mol %) Magnesium numbers of clinopyroxenes for the mafic cumulate rocks from the South of Kahramanmaraş. MORB and arc related gabbro fields are from Burns, 1985. The Mersin ophiolite trend is from Parlak et al., 1996, Pozantı-Karsantı ophiolite trend is from Parlak et al., 2000, Kızıldağ ophiolite trend is from Bağcı et al. 2005 and Tekirova ophiolite trend is from Bağcı et al., 2006

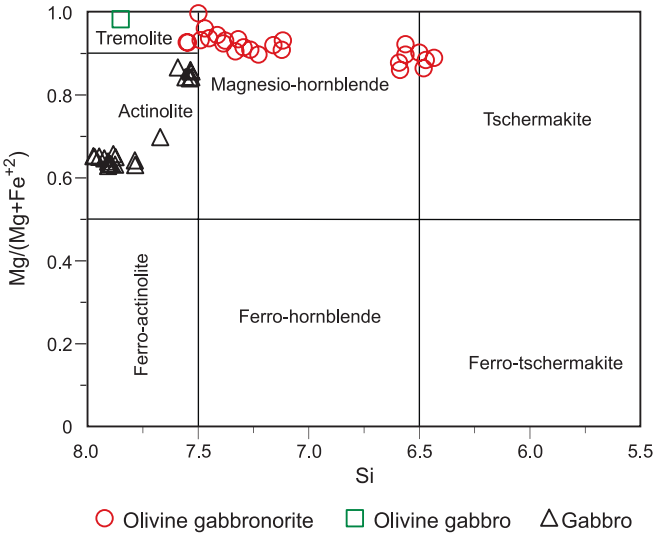

Fig. 15. Amphibole Classification diagram (after Leake et al., 1997).

Bağcı et al., 2005, 2008; Bağcı and Parlak, 2009; Dilek and Flower, 2003).

Bağcı (2013) suggested a distinct magma generation for the ophiolitic rocks from Kahramanmaraş region. According to this study, the ultramafic-mafic cumulates were formed in a suprasubduction zone tectonic setting, whereas the isotropic gabbros were subdivided into two groups as formed in SSZ tectonic setting and OIB-type magmatic sequences formed in a within-plate oceanic setting. The mafic cumulate rocks from the Kahramanmaraş region show REE and spider patterns as Low-Ti tholeiites and (Fig. 7a,b).

Ophiolites have been divided into two groups as high-Ti and low-Ti ophiolite types by making discrimination by using the fractionation trends of both gabbroic rocks and lavas and dykes (Miyashiro, 1973, 1975; Serri, 1980). While the high-Ti ophiolites show typical characteristics of MORB-like magmas the low-Ti ophiolites show a wide range of compositioal spectrum from mid ocean ridge basalts to island arc tholeiites and boninite-like magmas (Serri, 1980). As in the previous study by Serri (1980); rather than to use overlying dikes and lavas, using the cumulate gabbros is more effective for testing the type of ophiolite due to their less altered nature. In the TiO_2 vs MI (mafic index) diagram, the cumulate gabbroic rocks from Kahramanmaraş region are plotted in the field of low-Ti ophiolites (Fig. 6), and with the evaluation of other tectonomagmatic discriminaton diagram it is clearly seen that the mafic cumulate rocks from the southern part of Kahramanmaraş region show typical characteristics of the ophiolite formed in a suprasubduction zone tectonic setting with island arc tholeiitic magma source.

In conclusion;

Although the ophiolitic rocks that emplaced onto the Arabian passive margin in Late Cretaceous are incomplete and dismembered, except sheeted dykes and volcanics, they display Penrose-type ophiolite pseudostratigraphy such as the mantle tectonites, the ultramafic cumulates, the mafic cumulates, and isotropic gabbros. They are tectonically underlain by thin sheet of metamorphic sole rocks that mark the initiation of emplacement of oceanic lithosphere from the southern branch of Neotethys.

According to mafic Index (MI) and TiO_2 contents, the mafic cumulates of the ophiolite from the southern part of Kahramanmaraş can be classified as Low-Ti gabbro, suggesting derivation from a depleted magma source that is typical for the SSZ-type environment.

The mineral chemistry of the cumulate rocks indicates a low-pressure environment for the magma fractionation process during the crystallisation of main phases.

The presence of highly magnesian olivines (Fo_{82-78}) and pyroxenes ($Mg\#_{80-62}$) as well as highly calcic plagioclases (An_{97-82}) in the cumulates, indicates an intra-oceanic subduction-related tectonic environment for their generation.

The whole rock geochemical features of the cumulate rocks suggest that they were derived from a low-Ti island arc tholeiitic magma in a supra-subduction zone (SSZ) tectonic environment during the closure of the southern branch of Neotethyan oceanic basin in Late Cretaceous.

The presence of amphibole mineral in the cumulate gabbros indicates hydrous condition at the time of their magmatic differentiation and confirms the subduction-related setting for the generation of the crust.

ACKNOWLEDGEMENTS

This work is a part of MSc study of Mehmet Tanırlı. Financial support from Kahramanmaraş Sütçü İmam University Research Foundation (Project No: 2011/7-11YLS) is greatly acknowledged. We would like to thank Friedrich Koller for performing electron microprobe analyses at Vienna University (Austria). We are thankful to Yusuf Kaan Kadıoğlu and Bahattin Güllü for their kind help on performing major-trace element analyses at Ankara University. Two anonymous reviewers are thanked for their helpful reviews that improved the quality of the present paper. We are grateful to Osman Parlak for thoughtful discussions on petrology and significance of the Turkish ophiolites.

REFERENCES

Aktaş G., Robertson A. H. F. The Maden complex, SE Turkey: evolution of a Neotethyan continental margin // The geological evolution of the Eastern Mediterranean / Eds. J. E. Dıxon & A. H. F. Robertson. Geol. Soc. London, Spec. Publ., 1984, v. 17, p. 375–402.

Alabaster T., Pearce J. A. & Malpas J. The volcanic stratigraphy and petrogenesis of the Oman ophiolite complex // Contr. Miner. Petrol., 1982, v. 81, p. 168–183.

Al-Rıyamı K., Robertson A. H. F., Dixon J. & Xenophontos C. Origin and emplacement of the Late Cretaceous Baer-Bassit ophiolite and its metamorphic sole in NW Syria // Lithos, 2002, v. 65, p. 225–260.

Arculus R. J., Powel R. 1986. Source component mixing in the regions of arc magma generation // J. Geophys. Res., 1986, v. 91 (B6), p. 5913–5926.

Arculus R. J., Wills K. J. A. The petrology of plutonic blocks and inclusions from the Lesser Antilles Island Arc // J. Petrol., 1980, v. 21, 743–799.

Atan O. Geology of the Amanos Mountains (Egribucak-Karacaoren-Ceylanli-Dasevleri) // Maden Tetkik ve Arama Enstitüsü Yayınlarından 139, 1969.

Bağcı U. Kızıldağ (Hatay) ve Tekirova (Antalya) Ofiyolitlerinin Jeokimyası ve Petrolojisi. Doktora Tezi, Çukurova Üniversitesi Fen Bilimleri Enstitüsü, (Yayınlanmamış), 2004.

Bağcı U. The geochemistry and petrology of the ophiolitic rocks from the Kahramanmaraş region, Southern Turkey // Turkish J. Earth Sci., 2013, v. 22, p. 1–27.

Bağcı U., Parlak O. Petrology of the Tekirova (Antalya) ophiolite (Southern Turkey): evidence for diverse magma generations and their tectonic implications during Neotethyan subduction // Int. J. Earth Sci., 2009, v. 98, p. 387–405.

Bağcı U., Parlak O., Hoeck V. Whole-rock mineral chemistry of cumulates from the Kızıldağ (Hatay) Ophiolite (Turkey): Clues for multiple magma generation during crustal accretion in the Southern Neotethyan Ocean // Miner. Mag., 2005, v. 69(1), p. 53–76.

Bağcı U., Parlak O., Hoeck V. Geochemical character and tectonic environment of ultramafic to mafic cumulates from the Tekirova (Antalya) ophiolite (southern Turkey) // Geol J., 2006, v. 41, p. 193–219.

Bağcı U., Parlak O., Hoeck V. Geochemistry and tectonic environment of diverse magma generations forming the crustal units of the Kızıldağ (Hatay) ophiolite southern Turkey // Turkish J. Earth. Sci., 2008, v. 17, p. 43–71.

Barth T. F. W. Theoretical petrology. John Wiley and Sons, New York, 2013, 416 p.

Beccaluva L., Serri G. Boninitic and low-Ti subduction-related lavas from intraoceanic arc-backarc systems and low-Ti ophiolites: a reappraisal of their petrogenesis and original tectonic setting // Tectonophysics, 1988, v. 146, p. 291–315.

Beccaluva L., Ohnenstetter D., Ohnenstette M., Paupy A. Two magmatic series with island arc affinities within the Vourinos ophiolite // Contr. Miner. Petrol., 1984, v. 85, p. 253–271.

Beccaluva L., Macciotta G., Piccardo G. B. O. Clinopyroxene composition of ophiolite basalts as petrogenetic indicator // Chem. Geol., 1989, v. **77**, p. 165–182.

Beccaluva L., Coltorti M., Giunta G., Siena F. Tethyan vs Cordilleran ophiolites: a reappraisal of distinctive tectono-magmatic features of suprasubduction complexes in relation to the subduction mode // Tectonophysics, 2004, v. 393, p. 163–174.

Beccaluva L., Coltorti M., Saccani E., Siena F. Magma generation and crustal accretion as evidenced by supra-subduction ophiolites of the Albanide–Hellenid Subpelagonian zone // The Island Arc, 2005, v. 14, p. 551–563.

Bedard J., Lauziere K., Tremblay A., Sangster A. Evidence for forearc seafloor spreading from the Betts Cove ophiolite, Newfoundland: oceanic crust of boninitic affinity // Tectonophysics, 1998, v. 284, p. 233–245

Berger S., Cochrane D., Simons K., Savov I., Ryan J. G., and Peterson V. L. Insights from rare earth elements into the genesis of the Buck Creek Complex, Clay County, NC // Southeastern Geol., 2001, v. 40, №3, p. 201–212.

Beyarslan M., Bingol A.F. Petrology of a supra-subduction zone ophiolite (Elazığ, Turkey) // Can. J. Earth Sci., 2000, v. 37, p. 1411–1424.

Boulton S. J., Robertson A. H. F. The Neogene–Recent Hatay Graben, South Central Turkey: graben formation in a setting of oblique extension (transtension) related to postcollisional tectonic escape // Geol. Mag., 2008, v. 145, p. 800–821.

Boulton S. J., Robertson A. H. F., Ünlügenç U. C. 2006. Tectonic and sedimentary evolution of the Cenozoic Hatay Graben, Southern Turkey: a two-phase, foreland basin then transtensional basin model // Tectonic development of the Eastern Mediterranean region / Eds. A. H. F. Robertson, D. Mountrakıs. Geol. Soc. London, Spec. Publ., v. 260, p. 613–634.

Boynton W. V. 1984. Geochemistry of the rare earth elements: meteorite studies // Rare earth element geochemistry / Ed. P. Henderson. Elsevier, 1984, p. 63–114.

Burns L. E. The Border Ranges ultramafic and mafic complex, south-central Alaska: cumulate fractionates of island-arc volcanics. Can // J. Earth Sci., 1985, v. 22, p. 1020–1038.

Coleman R. G. Emplacement and metamorphism of ophiolites // Ofioliti, 1977, v. 2, p. 41–74.

Collins A., Robertson A. H. F. Processes of Late Cretaceous to Late Miocene episodic thrust-sheet translation in the Lycian Taurides, SW Turkey // J. Geol. Soc., 1998, v. 155, p. 759–772.

Debari S. M., Coleman R. G. Examination of the deep levels of an island arc: Evidence from the Tonsina Ultramafic-Mafic Assemblage, Tonsina, Alaska // J. Geophys. Res, 1989, v. 94, p. 4373–4391.

Dilek Y., Flower M. F. J. Arc-trench rollback and forearc accretion: 2. A model template for ophiolites in Albania, Cyprus, and Oman // Geol. Soc. London, Spec. Publ., 2003, v. 218, p. 43–68.

Dubertret L. Géologie des roches vertes du nord-ouest de la Syrie et du Hatay (Turquie). Notes Mém Moyen-Orient, 1955, v. 6, p. 227.

Elthon D. Petrology of the gabbroic rocks from the Mid-Cayman Rise spreading center // J. Geophys. Res., 1987, v. 92, p. 658–682.

Elthon D., Casey J. F., Komor S. Mineral chemsitry of ultramafic cumulates from the North Arm Mountain Massif of the Bay of Island Ophiolite: Evidence of high pressure crystal fractionation of oceanic basalts // J. Geophys. Res, 1982, v. 87, p. 8717–8734.

Elthon D., Casey J. F., Komor S. 1984. Cryptic mineral chemistry variations in a detailed traverse through the cumulate ultramafic rocks of the North Arm Mountain Massif of the Bay of Island Ophiolite, Newfoundland // Ophiolites and oceanic lithosphere / Eds. I. G. Gass, S. J. Lippard, A. W. Shelton. London, Blackwell, 1984, p. 83–97.

Erdoğan T. Gölbaşı Yöresinin Jeolojisi. Turkish Petroleum Company Report no. 229, 1975.

Floyd P. A., Goncuoğlu M. C., Winchester J. A., Yalınız M. K. Geochemical character and tectonic environment of Neotethyan ophiolitic fragments and metabasites in the Central Anatolian Crystalline Complex, Turkey // Tectonics and magmatism in Turkey and the surroundings area / Eds. E. Bozkurt, J. A. Winchester, J. D. A. Piper. Geol. Soc. London, Spec. Publ., 2000, v. 173, p. 183–202.

Foden J. D. The petrology of calc-alkaline lavas of Rindjami Volcano, East Sunda Arc: Model for island arcs // J. Petrol., 1983, v. 24, p. 98–130.

Fujimaki H. Fractional crystallization of the Basaltic Suite of Usa Volcano, Southwest Hokkaido, Japan, and its relationships with the associated Felsic Suite // Lithos, 1986, v. 19, p. 129–140.

Gass I. G. Is the Troodos Massif of Cyprus a fragment of Mesozoic ocean floor? // Nature, 1968, v. 220, 39–42.

Gass I. G. Ophiolites and oceanic lithosphere // Ophiolites—oceanic crustal analogues. Proceedings of Troodos Ophiolite Symposium-1987, Cyprus / Eds. J. Malpas, E. Moores, A. Panayiotou, C. Xenophontos. 1990, p. 1–10.

Gnos W., Peters T. K-Ar ages of the metamorphic sole of the Semail ophiolite: implications for ophiolite cooling history // Contr. Miner. Petrol., 1993, v. 113, p. 325–332.

Görür N., Oktay F. Y., Seymen İ., Şengör A. M. C. Palaeotectonic evolution of the Tuzgölü Basin Complex, Central Turkey: Sedimentary record of a Neotethyan closure // The geological evolution of the Eastern Mediterranean / Eds. J. E. Dıxon, A. H. F. Robertson. Geol. Soc. London, Spec. Publ., 1984, v. 17, p. 467–482.

Gust D. A., Johnson R. W. Amphibole bearing cumulates from Boisa island, Papua New Guinea: evaluation of the role of fractional crystallization in an andesitic volcano // J. Geol., 1981, v. 89, p. 219–232.

Gül M. Kahramanmaraş Bölgesinin Jeolojisi ve Petrol Olanakları. TPAO Rapor No. 2359, Ankara, 1987.

Gül M. A. Kahramanmaras Yoresinin Jeolojisi, Hacettepe Universitesi, Doktora tezi, 2000, 304 s.

Hebert R. & Laurent R. Mineral chemistry of the plutonic section of the Troodos ophiolite: New constraints for genesis of arc-related ophiolites // Ophiolites—oceanic crustal analogues / Eds. J. Malpas, E. Moores, A. Panayiotou, C. Xenophontos. Proceedings of Troodos Ophiolite Symposium-1987, Cyprus, 1990, p. 149–163.

Hoeck V., Koller F., Meisel T., Onuzi K., Kneringer E. The Jurassic South Albanian ophiolites: MOR-vs. SSZ-type ophiolites // Lithos, 2002, v. 65, p. 143–64.

Inwood J., Morrıs A., Anderson M. W., Robertson A. H. F. Successive structural events in the Hatay ophiolite of southeast Turkey: distinguishing oceanic, emplacement and post-emplacement phases of faulting // Tectonophysics, 2009, v. 473, 208–222.

Irvıne T. N., Baragar W. R. A. A Guide to the Chemical Classification of the Common Volcanic Rocks // Can. J. Earth Sci., 1971, v. 8, p. 523–548.

Jameison R.A. The St. Anthrony complex, northwestern Newfoundland: petrologic study of the relationship between a peridotite sheet and its dynamothermal aureole // PhD Thesis, Mernorial University Newfoundland, 1979.

Leake E.B., Wooley A. R., Arps C.E.S., Birch W. D., Gilbert M. C., Grice J. D., Hawthorne F.C., Kato A., Kisch H. J., Krivovichev V. G., Linthout K., Laird J., Mandarino J., Maresch W. V., Nickhel E. H., Rock N. M. S., Schumacher J. C., Smith D. C., Stephenson N. C. N., Ungaretti L., Whittaker E. J. W., Youzhi G. Nomenclature of amphiboles // Eur. J. Miner. , 1997, v. 9, 623–651.

Lytwyn J. N., Casey J. F. The geochemistry of postkinematic mafic dyke swarms and subophiolitic metabasites, Pozantı-Karsantı ophiolite, Turkey: evidence for ridge subduction // Geol. Soc. Amer. Bull., 1995, v. 107, 830–850.

Malpas J., Langdon G. Petrology of Upper Pillow Lava Suite, Troodos Ophiolite, Cyprus // Geol. Soc. London, Spec. Publ., 1984, v. 13, p. 155–167.

Medaris L. G. High-pressure peridotites in south-western Oregon // Bull. Geol. Soc. Amer., 1972, v. 83, p. 41–58.

Meffre S., Aitchison J., Crawford A. J. Geochemical evolution and tectonic significance of boninites and tholeiites from the Koh ophiolite, New Caledonia. Tectonics, 1996, v. 15, p. 67–83.

Miyashiro A. The Troodos ophiolitic complex was probably formed in an island arc // Earth Planet. Sci. Lett., 1973, v. 19, p. 218–224.

Miyashiro A. 1975, Classification characteristics and origin of ophiolites // J. Geol., 1975, v. 83, p. 249–281.

MTA 1/500.000 Türkiye Jeoloji Haritası / General Directorate of Mineral Research and Exploration, Ankara, Turkey, 2002.

Nicolas A. Structures of ophiolites and dynamics of oceanic lithosphere. Springer, Dordrecht, Netherlands, 1989, p. 261–274.

Okay A. I. Geology of the Menderes Massif and the Lycian nappes south of Denizli, western Taurides // Bull. Miner. Res. Explor., 1989, v. 109, p. 37–51.

Okay A. I., Tüysüz O. Tethyan sutures of northern Turkey // The Mediterranean basins: Tertiary extensions within the Alpine Orogen / Eds. B. Durand, L. Jolıvet, F. Horvath, M. Seranne. Geol. Soc. London, Spec. Publ., 1999, v. 156, p. 474–515.

Panjasawatwong Y., Danyushevsky L. V., Crawford A. J., Harris K. L. An experimental study of the effects of melt composition on plagioclase-melt equilibria at 5 and 10 kbars: implications for the origin of magmatic high-An plagioclase // Contr. Miner. Petrol., 1997, v. 118, p. 420–432.

Parlak O. Geochemistry and geochronology of the Mersin ophiolite within the eastern Mediterranean tectonic frame. PhD Thesis, Terre et Environnement, v. 6, University of Geneva, 1996.

Parlak O., Delaloye M. Precise $^{40}Ar/^{39}Ar$ ages from the metamorphic sole of the Mersin ophiolite (Southern Turkey) // Tectonophysics, 1999, v. 301, p. 145–158.

Parlak O., Delaloye M., Bingöl E. Origin of sub-ophiolitic metamorphic rocks beneath the Mersin ophiolite, Southern Turkey // Ofioliti, 1995, 20(2), p. 97–110.

Parlak O., Delaloye M., Bingöl E. Mineral chemistry of ultramafic and mafic cumulates as an indicator of the arc-related origin of the Mersin ophiolite (southern Turkey) // Geologische Rundschau, 1996, v. 85, p. 647–661.

Parlak O., Hoeck V., Delaloye M. Suprasubduction zone origin of the Pozanti-Karsanti ophiolite (southern Turkey) deduced from whole-rock and mineral chemistry of the gabbroic cumulates // Tectonics and magmatism in Turkey and the surrounding area / Eds. E. Bozkurt, J. A. Winchester, J. D. A. Piper. Geol. Soc. London, Spec. Publ., 2000, v. 173, p. 219–234.

Parlak O., Hoeck V., Delaloye M. The suprasubduction zone Pozantı–Karsantı ophiolite, southern Turkey: evidence for high-pressure crystal fractionation of ultramafic cumulates // Lithos, 2002, v. 65, p. 205–224.

Parlak O., Hoeck V., Kozlu H., Delaloye M. Oceanic crust generation in an island arc tectonic setting, SE Anatolian Orogenic Belt (Turkey) // Geol. Mag., 2004, v. 141, p. 583–603.

Parlak O., Rızaoğlu T., Bağcı U., Karaoğlan, F., Hoeck V. Geochemistry of ophiolites in the Southeast Anatolia, Turkey // Tectonophysics, 2009, v. 473 (1–2), p. 173–187.

Parlak O., Karaoğlan F., Rızaoğlu T., Nurlu N., Bağcı U., Hoeck V., Öztüfekçi Önal A., Kürüm S., Topak Y. Petrology of the İspendere (Malatya) ophiolite from the Southeast Anatolia: implications for the Late Mesozoic evolution of the southern Neotethyan ocean // Geol. Soc. London, Spec. Publ., 2012, v. 372, p. 219–247.

Peacock S. M. and Norris P. J. Metamorphic evolution of the central metamorphic belt, Klamath Province, California: an inverted metamorphic gradient beneath the Trinity peridotite // J. Metamorph. Geol., 1989, v. **7**, p. 19l–209.

Pearce J.A. Role of the subcontinental lithosphere in magma genesis at active continental margins // Continental basalts and mantle xenoliths / Eds. C. J. Hawkesworth, M. J. Norry. Shiva Publishing, Cheshire, 1983, pp. 230–249.

Pearce J. A., Alabaster T., Shelton A. W., Searle M. P., Vine, F. J., Smith A.G. The Oman ophiolite as a Cretaceous arc-basin complex, evidence and implications // Philos. Trans. R. Soc. London, Ser. A, 1981, v. 300, p. 299–317.

Pearce J. A., Lippard S. J., Roberts S. Characteristics and tectonic significance of suprasubduction zone ophiolites // Marginal basin geology / Eds. B. P. Kokelaar, M. F. Howells. Geol. Soc. London, Spec. Publ., 1984, v. 16, p. 77–94.

Pe-Piper G., Tsikouras B., Hatzıpanagiotou K. Evolution of boninites and island-arc tholeiites in the Pindos ophiolite, Greece // Geol. Mag., 2004, v. 141, p.455–469.

Pişkin Ö., Delaloye M., Moritz R., Wagner J. J. Geochemistry and geothermometry of the Hatay complex Turkey: implication for genesis of the ophiolite sequence // Ophiolites—oceanic crustal analogues. Proceedings of Troodos Ophiolite Symposium-1987 / Eds. J. Malpas, E. Moores, A. Panayiotou, C. Xenophontos. Geological Survey, Cyprus, 1990, p. 329–337.

Rızaoğlu T. Baskil - Sivrice (Elazığ) Arasında Yüzeyleyen Tektonomagmatik Birimlerin Jeokimyası ve Petrografisi. Doktora Tezi, Çukurova Üniversitesi, Fen Bilimleri Enstitüsü, Jeoloji Mühendisliği Anabilim Dalı Balcalı-Adana (Yayınlanmamış), 2006.

Rızaoğlu T., Parlak O., Hoeck V., İşler F. Nature and significance of Late Cretaceous ophiolitic rocks and its relation to the Baskil granitoid in Elazığ region, SE Turkey // Tectonic development of the Eastern Mediterrranean region / Eds. A. H. F. Robertson, D. Mountrakis. Geol. Soc. London, Spec. Publ., 2006, v. 260, p. 327–350.

Robertson A. H. F. Overview of the genesis and emplacement of Mesozoic ophiolites in the Eastern Mediterranean Tethyan region // Lithos, 2002, v. 65, p. 1–67.

Robertson A. H. F., Ustaömer T., Parlak O., Ünlügenç U. C., Taslı K., İnan N. The Berit transect of the Tauride thrust belt, S. Turkey: late Cretaceous–Early Cenozoic accretionary/collisional processes related to closure of the southern Neotethys // J. Asian Earth Sci., 2006, v. 27, p. 108–145.

Robertson A. H. F., Parlak O., Rızaoğlu T., Ünlügenç U. C., İnan N., Taslı K., Ustaömer T. Tectonic evolution of the South Tethyan ocean: evidence from the Eastern Taurus Mountains (Elazığ region, SE Turkey) // Deformation of continental crust / Eds. A. C. Rıes, R. W. H. Butler, R. H. Graham. Geol. Soc. London, Spec. Publ., 2007, v. 272, p. 231–270.

Rollinson H. Using geochemical data: Evaluation, presentation, interpretation. Longman Group, UK, 1993, 352 pp.

Saccani E., Photiades A. Mid-ocean ridge and supra-subduction affinities in the Pindos Massif ophiolites (Greece): implications for magma genesis in a protoforearc setting // Lithos, 2004, v. 73, p. 229–253.

Saccani E., Photiades A. Petrogenesis and tectonomagmatic significance of volcanic and subvolcanic rocks in the Albanide–Hellenide ophiolitic mélanges // The Island Arc, 2005, v. 14, p. 494–516.

Sandeman H. A., Chen Y., Clarck A. H., and Farrar E. Constraints on the *P-T* conditions and age of emplacement of the Lizard ophiolite, Cornwall: arnphibole-plagioclase thermobarometry and $^{40}Ar/^{39}Ar$ geochronology of basal amplribolites // Can J. Earth Sci., 1995, v. 32, p. 261–272.

Şengör A. M. C., Yılmaz Y. Tethyan evolution of Turkey: Plate tectonic approach // Tectonopysics, 1981, v. 75, p. 181–241.

Serri G. The petrochemistry of ophiolite gabbroic complexes. A key for the classification of ophiolites into Low-Ti and High-Ti types // Earth Planet. Sci. Lett., 1980, v. 52, p. 203–212.

Sisson T.W., Grove T.L. Experimental investigations of the role of H_2O in calc-alkaline differentiation and subduction zone magmatism // Contr. Miner. Petrol., 1993, v. 113, p. 143–166.

Smellie J. L., Stone P., Evans J. Petrogenesis of boninites in the Ordovician Ballantrae Complex ophiolite, southwestern Scotland // J. Volcanol. Geotherm. Res., 1995, v. 69, p. 323–342

Spandler C., Hermann J., Arculus R., Mavrogenes J. Redistribution of trace elements during prograde metamorphism from lawsonite blueschist to eclogite facies; implications for deep subduction processes // Contr. Miner. Petrol., 2003, v. 146, p. 205–222.

Stern R. J. On the origin of andesite in the Northern Mariana Islands: Implications from Agrigan // Contr. Miner. Petrol, 1979, v. 68, p. 207–219.

Sun S. S., Mcdonough W. F. Chemical and isotopic systematics of ocean basalts: Implications for mantle composition and processes // Magmatism in the ocean basins / Eds. A. D. Saunders, M. J. Norry. Geol. Soc. London, Spec. Publ., 1989, v. 42, p. 313–46.

Sungurlu O. VI. Bölge kuzeyinin jeolojisi ve petrol imkanları, Türkiye II. Petrol Kong. Teb., Ankara, 1974, p. 85–107.

Tekeli O., Erendil M. Geology and petrology of the Kızıldağ Ophiolite (Hatay) // Bulletin of Mineral Research and Exploration Institute of Turkey, 1986, v. 21, p. 21–37.

Terlemez H. Ç. İ., Şentürk K., Ateş Ş., Sümengen M., Oral A. Gaziantep Dolayının ve Pazarcık-Sakçagöz-Kilis-Elbeyli-Oğuzeli Arasının jeolojisi. Maden Tetkik ve Arama Genel Müdürlüğü (MTA) Yayını, No. 9526, 1992.

Tuna D. VI. Bölge litostratigrafi birimleri adlamasının açıklayıcı raporu : TPAO. Rapor no. 813, 13 s., Ankara (Yayınlanmamı), 1973.

Wallin E. T., Metcalf R. V. Supra-subduction zone ophiolites formed in an extensional forearc: Trinity Terrane, Klamath Mountains, California // J. Geol., 1986, v. 106, p. 591–608.

Williams H., Smyth W. R. Metamorphic aureoles beneath ophiolite suites and Alpine peridotites: tectonic implications with west Newfoundland examples // Amer. J. Sci., 1973, v. 273, p. 594–621.

Wood D. A., Joron J. L., Treuil M. A reappraisal of the use of trace elements to classify and discriminate between magma series erupted in different tectonic settings // Earth Planet. Sci. Lett., 1979, v. 45, p. 326–336.

Yalçın N. Doğu Anadolu yarılımının Türkoğlu-Karaağaç (Kahramanmaraş) arasındaki kesiminin özellikleri ve bölgedeki yerleşim alanları Altınlı Simp., özel sayı, TJK, İstanbul Üniversitesi Yerbilimleri Fakültesi Jeoloji Bölümü, 1979, p. 49–55,

Yalınız K. M., Floyd P., Goncuoğlu M. C. Suprasubduction zone ophiolites of Central Anatolia: geochemical evidence from the Sarikaraman ophiolite, Aksaray, Turkey // Miner. Mag., 1996, v. 60, p. 697–710.

Yıldırım N., İlhan S., Yıldırım E., Dönmez C. Ormanbaşı Tepe (Sincik-Adıyaman) Cu cevherleşmesinin Jeolojisi, Jeokimyası ve Jenetik Özellikleri // MTA Dergisi, 2012, v. 144, 75–102.

Yılmaz Y. New evidence and model on the evolution of the Southeast Anatolian orogen // Bull. Geol. Soc. Amer., 1993, v. 105, p. 251–271.

Yılmaz Y., Demirkol C., Yalçın N., Yiğitbaş E., Gürpınar O.,Yetiş C., Günay Y., Sarıtaş B. Amanos Dağlarının Jeolojisi, II Ofiyolit. İstanbul Teknik Üniversitesi Mühendislik Fakültesi Publication 351, 1984.

Yılmaz Y., Gürpınar O., Kozlu H., Gül M. A., Yiğitbaş E., Yıldırım M., Genç C., Keskin M. Kahramanmaraş Kuzeyinin Jeolojisi (Andırın-Berit-Engizek-Nurhak-Binboğa Dağları). Türkiye Petrolleri A. O. Rap, No: 2028, 1987, 218s.

Yılmaz Y., Yiğitbaş E., Genc Ş.C. Ophiolitic and metamorphic assemblages of Southeast Anatolia and their significance in the geological evolution of the orogenic belt // Tectonics, 1993, v. 12, p. 1280–1297.

Yılmaz Y., Tüysüz O., Yiğitbaş E., Genc S. C., Şengör A. M. C. Geology and tectonic evolution of the Pontides // Regional and petroleum geology of the Black Sea and surrounding regions / Ed. A. G. Robınson. Amer. Assoc. Petrol. Geol. Mem., 1997, v. 68, p. 183–226.

Yibas B., Reimold W. U., Anhaeusser C. R., Koeberl C. Geochemistry of the mafic rocks of the ophiolitic fold and thrust belts of southern Ethiopia: constraints on the tectonic regime during the Neoproterozoic (900–700 Ma). Precambrian Res., 2003, v. 121 (3/4), p. 157–183.

Yogodzinski G. M., Volynets O. N., Koloskov A. V., Seliverstov N. I., Matvenkov V. V. Magnesian andesites and the subduction component in strongly calc-alkaline series at Piip volcano, far western Aleutians // J. Petrol., 1993, v. 35, p. 163–204.

Yoldemir O. Gölbaşı (Adıyaman) Güneyindeki Alanda İzlenen Haydarlı Formasyonunun (Üst Kretase) Sedimantolojisi ve Ortamsal Yorumu // 7 Türkiye Petrol Kongresi, Bildiriler, p. 192–202, 1987.

Рекомендована к печати 29 января 2016 г.
А.Э. Изохом

Поступила в редакцию 31 марта 2015 г.,
после доработки — 6 ноября 2015 г.